

# Evaluation and Multi-Criteria Optimization of Surface Roughness, Deviation From Dimensional Accuracy and Roundness Error in Drilling CFRP/Ti6Al4V Stacks

**Ali Riza Motorcu**

Professor  
Çanakkale Onsekiz Mart University  
Faculty of Engineering  
Turkey

**Ergün Ekici**

Associate Professor  
Çanakkale Onsekiz Mart University  
Faculty of Engineering  
Turkey

*In this study, machinability tests were carried out to investigate the effects of control factors (cutting tool geometry, cutting speed, and feed rate) on the surface roughness ( $R_a$ ), deviation from dimensional accuracy ( $Da_{dev}$ ), roundness error ( $Re$ ) in drilling CFRP/Ti6Al4V mixed metallic stack and to determine the optimum levels of drilling parameters. The effects of each control factor and their interactions on three quality characteristics were analyzed, and their levels were single-objectively optimized for each component material by the Taguchi method. The material has components (CFRP and Ti6Al4V) with essentially different properties (mechanical, physical, machinability). Single-objective optimization has limited usability as the drilling must be performed in one through both layers. Therefore, in an additional step, the optimum levels of the control factors were determined by optimizing multi-objective with the Additive Ratio Assessment (ARAS) method. Higher  $R_a$ ,  $Da_{dev}$ , and  $Re$  values were obtained on the CFRP component compared to the Ti6Al4V component. The CFRP/Ti6Al4V stack should be drilled with a nano fire coated carbide drill (T3) at medium cutting speed and high feed rate to achieve minimum  $R_a$ ,  $Da_{dev}$ , and  $Re$  values in one go.*

**Keywords:** CFRP/Ti6Al4V hybrid metallic stack, Drilling, Additive Ratio Assessment (ARAS), Surface roughness, Deviation from dimensional accuracy, Roundness error

## 1. INTRODUCTION

Stacks of titanium alloys and carbon fiber reinforced polymers (CFRP) are advanced functional structures commonly used in the aerospace industry because of their enhanced mechanical properties and flexibility for structural design. Although CFRP/Ti6Al4V stacks are produced in desired geometries, drilling operations are needed in assembly processes [1-5]. Drilling constitutes approximately 1/3 of the machining operations and is usually applied as a finishing operation. The chip formation is in a closed area, making it difficult to control the drilling process. In drilling operations, vibrations in the drill and workpiece, tool wear, chips sticking on the tool, tool geometry, feed rate, cutting speed, workpiece material properties, and chips affect surface roughness. Other important quality indicators in drilling operations are the dimensional accuracy of the hole and the roundness error. In drilling operations, the hole diameters must be at the nominal diameter. However, deviations from the nominal diameter occur in drilling operations. Especially in the drilling of stack materials, deviations from this nominal diameter may

also differ between the components due to each component's different properties that make up the stack. In this case, it becomes even more difficult to ensure the dimensional accuracy of the hole diameter.

CFRP/Ti6Al4V composite/metal stacks, widely used in aerospace components due to their high strength/weight ratio, are overlapped, drilled together in one go, and then joined with screws. Therefore, CFRP and Ti6Al4V should be drilled under optimum machining conditions to achieve better hole quality when drilling through one step [6]. The cutting tool geometry significantly impacts the machinability of CFRP/Ti stacks. Current knowledge of machining CFRP/Ti6Al4V mixed metallic stacks is insufficient to guide their industrial application. Because the effect of various cutting conditions on hole damage, dimensional hole accuracy, and hole quality when machining CFRP/Ti alloy stacks has been little studied [7-11]. In the machinability studies, it has been observed that the effects of coating properties, number of teeth, and cutting parameters of carbide tools are frequently evaluated. In contrast, the effects of cutting tool geometry are examined in some limited studies. It has been reported in the literature that the cutting tool geometry has a significant effect on the delamination formation/damage in the drilling of CFRP and the hole quality in the drilling of Ti6Al4V alloy. The performance of current tool geometries, which are claimed to be very successful in drilling only CFRP

---

Received: April 2022, Accepted: June 2022  
Correspondence to: Prof. Dr Ali Riza MOTORCU  
Faculty of Engineering, ÇOMÜ  
Terzioğlu Campus, 17100, Çanakkale, Turkey  
E-mail: armotorcu@comu.edu.tr  
**doi:10.5937/fme2203441M**

© Faculty of Mechanical Engineering, Belgrade. All rights reserved

FME Transactions (2022) 50, 441-460 **441**

composites, on the drilling of CFRP/Ti6Al4V mixed metallic stacks should also be investigated. Therefore, studies on the machining of CFRP/Ti6Al4V mixed metallic stacks still maintain their importance and continue. Kourra et al. ensure the quality of the drilled holes by measuring the maximum diameter variation, roundness, and hole positioning in CFRP/Ti6Al4V stacks with X-ray computed tomography (CT) and image processing method and examining the entry delamination and exit burrs with image processing [2]. Xu et al., in their study investigating the relationship between cutting sequence strategy, drilling forces, hole damage, and surface morphology, stated that drilling from Ti to CFRP provides more advantages than drilling from CFRP to Ti for drilling CFRP/Ti stacks in one step [3]. Kolesnyk et al. investigated the drilling temperature, the phenomenon of thermal expansion of the drill tool, and hole accuracy. The study's results showed that the time delay factor varied from 5 (s) to 120(s), affecting the thermal-dependent properties of CFRP and leading to an increase in hole roundness [7]. In the study by Xu and El Mansori, the Ti/CFRP drilling strategy provided lower Ti burr lengths with more consistent hole diameters and much better surface quality. In contrast, the CFRP/Ti drilling strategy only reduced induced delamination [8]. Ekici and Motorcu investigated the effects of machining parameters and drilling strategy on surface roughness in drilling CFRP/Ti6Al4V metallic stacks. Two different drilling strategies, CFRP→Ti6Al4V and Ti6Al4V→CFRP, were used. According to the results, the surface roughness values of the holes in the CFRP drilling were higher, 81.13% on average, compared to the Ti6Al4V alloy. Compared to the CFRP→Ti6Al4V drilling strategy, the hole surface roughness was 49.55% larger on average in drilling with the Ti6Al4V→CFRP drilling strategy [9]. Xu et al. emphasized that chips cut from titanium affect the surface quality of the composite, and strict tool wear control is required to guarantee undamaged drilling of CFRP/Ti6Al4V stacks [10]. Xu and El Mansori report that when machining hybrid CFRP/Ti stacks with PCD tools, strict tool wear control must be applied to ensure excellent machined surface quality [11]. Kim et al. improved the machinability in hole quality parameters such as average hole size, average hole roundness, hole surface roughness and Ti exit burr, and drilling forces by using advanced AlCrN coated tools CFRP–Ti stacks [12]. In the study of Isbilir and Ghassemieh, the effects of cutting parameters on delamination and mean surface roughness in drilling CFRP tend to be similar to those in drilling Ti-6Al-4V [13]. A new step drill with a special margin structure is proposed for drilling Ti/CFRP stacks in the study of Zhang et al. [14]. Wang et al. investigated the effects of Ti on the hole quality of CFRP in helical milling of a CFRP/Ti laminate [15]. The study by Kayihan et al. investigated the effects of process parameters and stack order on thrust force, torque, and surface roughness [16]. In the study of Xu et al. on the drilling of CFRP/Ti6Al4V stacks under minimal lubrication (MQL) conditions, better surface morphologies and less titanium burr formation were obtained CFRP holes. Moreover, MQL provided better geometric accuracy

[17]. In Xu et al.'s study, the MQL application fails to minimize hole roundness errors in drilling CFRP/Ti6Al4V stacks [18]. In Akhil et al.'s study, the effects of machining parameters on thrust force and hole quality were also investigated in dry and MQL drilling of CFRP/Ti alloy stacks [19]. In the study of An et al., the Ti→CFRP drilling sequence was preferred in terms of drilled hole accuracy of CFRP/Ti stacks. In contrast, the CFRP→Ti drilling sequence was preferred to reduce delamination damages in practical engineering production [20]. Jia et al. introduce a new depth-of-cut drill structure to improve the drilling quality/accuracy of the Ti/CFRP stack [21]. In the study by Xu et al., it was determined that drilling from Ti to CFRP leads to higher shear temperatures of the composite, decreases the stacking thrust forces, improves the composite surface morphologies, and reduces the exit titanium burr heights [22]. Xu et al.'s study examining different cutting sequence strategies has allowed a better understanding of the machinability of CFRP/Ti6Al4V stacks [23]. Alonso et al. investigated the effect of flute number and stepped tip design [24]. In a study by Prisco et al., the effect of tool wear on the dimensional and geometric accuracy of machined holes was investigated in pecking drilling of CRFP and Ti stacks [25]. The surface integrity was evaluated by Kuo et al. Ti-6Al-4V/CFRP/Al-7050 stack was drilled using a CVD diamond coated tool [26]. Ekici et al. investigated the effects of drilling parameters and cutting tool coating conditions on thrust force, surface roughness, and delamination factor in drilling fiber-reinforced carbon-reinforced aluminum laminate composite. According to the study's results, the most effective factor on the surface roughness was the cutting tool coating state-cutting speed interaction with an additive ratio of 66.504 [27]. Pramanik and Littlefair analyzed the forces and torque, chip shapes, surface finish and geometry, tool material and tool wear to drill composite/metal stack, and the drilling mechanism of CFRP [28]. Shyha et al. analyzed hole quality/integrity after drilling titanium/CFRP/aluminum stacks under flood coolant and spray mist environments [29]. Ashmawi et al. investigated the effect of cutting parameters on surface roughness and burr formation during milling a stack of Ti and CFRP [30]. Chashchin et al. explained the effects of cutting parameters on hole accuracy in drilling hybrid stacks and offered suggestions for optimizing the cutting parameters [31]. Ekici et al. investigated the hole quality in the drilling of CARALL composite. In the study, the delamination factor calculation approaches of Chen, Davim, and Machado were also compared in terms of delamination damage on the hole entrance surface. The values closest to the nominal hole diameter were obtained with uncoated, TiN-TiAlN coated, and TiAl/TiAlSiMoCr coated carbide drills [32]. Kumar and Verma developed a robust hybrid module for multi-criteria optimization of machining performances for milling GO-doped Epoxy/CFRP composites. Spindle speed, feed rate, depth of cut, and GO wt percent were selected as process constraints. Minimum roughness, cutting force, and maximum metal-removal rate (MRR) were 0.730  $\mu\text{m}$ , 4.706 N, and 17.0484  $\text{mm}^3/\text{s}$ , respectively. According to the ANOVA results, spindle

speed and feed rate were determined as the most important parameters for the overall assessment value [33]. In the study conducted by Nan et al., an automatic drilling prototype was developed to investigate the quality properties of the CFRP layer in drilling CFRP/Ti stacks, and drilling experiments of single CFRP and CFRP/Ti stacks were designed to analyze the effect of titanium chip formation, respectively [34]. In the study by Wei et al., after the experiments performed with different drills in the drilling of CFRP/Ti alloy, it was determined that the effect of the cutting speed was low, while the hole quality had a strong correlation with the feed rate [35]. As it can be understood from the studies in the literature, most of the research is done experimentally, and the experimental results are evaluated with traditional methods. Determining the relationships between control factors and quality characteristics in research is essential. There are many output parameters (dependent variables) in determining the hole quality, which determines the machinability rate of a material, and the input parameters (control factors/independent variables) affect the hole quality at different rates. When a hole is drilled through a stack, all criteria/characteristics such as hole wall surface roughness, hole diameter dimensional accuracy, roundness error, etc., that define/determine the quality of that hole must be met simultaneously. Evaluating the quality characteristics of a hole as a whole can be achieved with multi-criteria optimization methods. However, there is no adequate study in the literature evaluating the machinability of Ti alloys, CFRP composites, and CFRP/Ti6Al4V mixed metallic stacks and using multi-objective optimization methods.

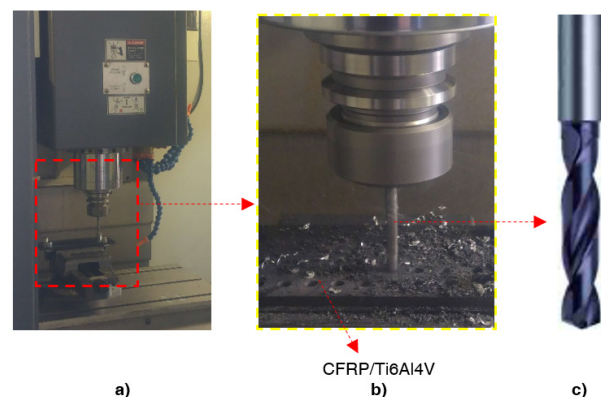
Therefore, this study has two aims. The first of these is to investigate the effects of control factors (cutting tool geometry, cutting speed, and feed rate) on the surface roughness ( $Ra$ ), deviation from dimensional accuracy ( $Da_{dev}$ ), roundness error ( $Re$ ) in drilling CFRP/Ti6Al4V mixed metallic stack and to determine the optimum levels of control factors. For achieving this aim, the effects of each control factor and their interactions on three quality characteristics were analyzed, and their levels were single-objectively optimized for each component material by the Taguchi method. The material has components (CFRP and Ti6Al4V) with essentially different properties (mechanical, physical, machinability). Single-objective optimization has limited usability as the drilling must be performed in one through both layers. Therefore, the second aim of this study is to determine the optimum levels of the control factors that simultaneously provide the minimum  $Ra$ ,  $Da_{dev}$ , and  $Re$  values by multi-objective optimization. The Additive Ratio Assessment (ARAS) method was used to achieve this. Thus, as a result of the systematic optimization studies carried out within the scope of this study, this deficiency in the literature was eliminated with results and findings with high accuracy and confidence levels. It is thought that the findings and results of this research will contribute to the formation and development of machinability databases of CFRP/Ti6Al4V mixed metallic stacks, will

be a source for scientific and academic studies in the field of manufacturing engineering and machinability, and will also benefit the use of machinability data needed by practitioners in industrial applications.

## 2. MATERIAL AND METHOD

### 2.1 CFRP/Ti6Al4V stack workpiece, cutting tools, and machinability tests

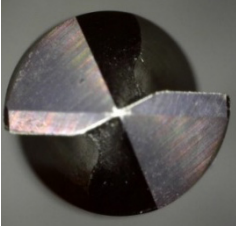
Machinability tests were carried out on a three-axis FALCO VMC 550 CNC vertical machining center (Fig. 1.a). CFRP/Ti6Al4V metallic stack material used as workpiece material consists of 5 mm thick Ti6Al4V alloy (Quality 5) and 5 mm thick CFRP plate produced by vacuum infusion method with 64% fiber and 36% resin content. In the CFRP composite sample production, two different woven carbon fabrics (4 Layers 245 gr/m<sup>2</sup> and 11 Layers 450 gr/m<sup>2</sup>) were used. Carbon fabrics were used as 2 layers of 245 gr/m<sup>2</sup> in the lowest row, 11 layers of 450 g/m<sup>2</sup> in the middle row, and 2 layers of 245 g/m<sup>2</sup> in the top row. The Ti6Al4V plates supplied with the CFRP plates were cut in 200x100x5 mm dimensions and stacked with a bolted connection (Fig. 1.b) [4, 5]. Drilling processes were carried out with coated carbide tools and without coolant (Fig. 1.c). Each hole is drilled with a new drill. Drilling experiments were carried out with the drilling strategy of starting drilling from the Ti plate (Ti6Al4V → CFRP) (Fig. 1.c).



**Figure 1. Drilling experiments: a) CNC vertical machining center, b) Workpiece, c) Cutting tool**

The geometry and properties of the drills used in the experiments are presented in Table 1. T1 coded tool manufactured by Guhring cutting tool company used in drilling tests, tip angle of 140°, body thinning  $\geq \text{Ø}3.0$  mm, lightened (free) cone, main cutting edge slightly concave, nano-Si with two protruding edges around the drill coated carbide drill. The cutting tool code T2 has a tip angle of 140° and two protruding edges around the drill. It is a nano-firex coated carbide drill with a concave main cutting edge, body thinning  $\geq \text{Ø}5.0$  mm, a lightened (free) cone, and sharp main cutting edges. T3 coded tool is a nano fire coated carbide drill with a tip angle of 140°, body thinning  $\geq \text{Ø}5.0$  mm, crystal surface end grinding, two protruding edges around it, and a straight main cutting edge form.

**Table 1. Geometry and technical properties of cutting tools**

		T1 (8524 6.000 RT 100 HF)	T2 (2475 6.00 RT 100 F)	T3 (5514 6.000 RT 100 U)
<b>Tool code and geometry</b>				
<b>Coating</b>	Code	Nano-Si	Nano-FIREX	Nano-FIREX
	Coating material	TiAlSiN	TiN-TiAlN	TiN-TiAlN
	Layer structure	Multilayer	Micro-Thin Multilayer	Micro-Thin Multilayer
	Thickness (µm)	4-6	1.5-4	1.5-4
	Nano hardness (HV 0.05)	5500	3800	3800
	Friction coefficient	0.55	0.5	0.5
<b>Geometric dimensions</b>	Body thinning (mm)	≥ Ø3.0	≥ Ø5.0	≥ Ø5.0
	Drill diameter (mm)		6	
	Total length (mm)		66	
	Flute length (mm)		28	
	Max. drilling depth (mm)		19	
	Shank length		36	
	Point angle (°)		140	

**2.2. Surface roughness (Ra), dimensional accuracy (Da\_dev), and roundness error (Re) measurements**

Surface roughness measurements were performed using Mitutoyo Surftest 201 surface roughness instrument. For each drilled hole, 5 surface roughness measurements were made at equal angles from the periphery of the hole surfaces. The measuring distance is set as ( $\lambda c$ )=2.5 mm. In order to define the surface roughness of the hole surfaces, the surface roughness average (Ra) values were taken as a basis. In this study, the deviation from dimensional accuracy (Da\_dev) is defined as the absolute value of the difference between the desired diameter value (drill diameter) and the measured

diameter (Da) value. The hole's roundness error (Re) is the difference between the largest and smallest radius measured from a given center point.

The roundness error (Re) in the hole indicates diametrical fluctuations on the hole surface. In this study, it is considered to determine the fluctuations on the hole surface by determining the differences between the largest and smallest radius measured by contacting the hole surface from 10 points at equal angles. In order to precisely determine the quality of the drilled holes, the upper surface of the part was taken as a reference, and dimensional accuracy and roundness error measurements were made at 1.5 mm, 3 mm, 6.5 mm, and 8 mm from this surface.

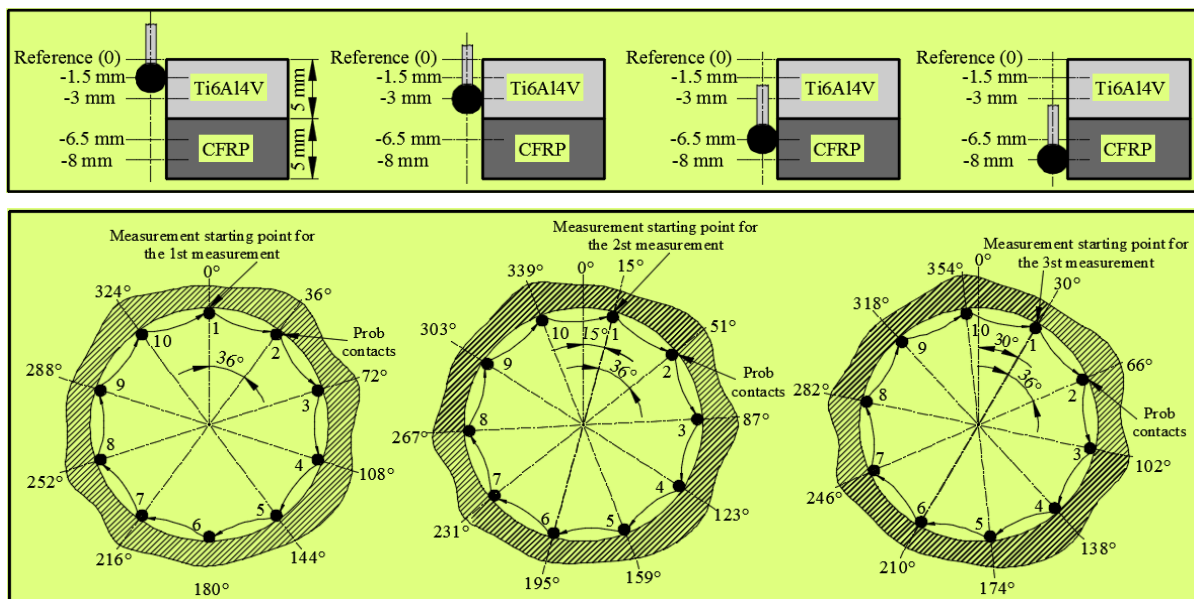


**Figure 2. Schematic representation of dimensional accuracy and roundness error measurement on CFRP/Ti6Al4V stack.**

For the first hole, the probe was first touched to a point on the hole surface at the height of 1.5 mm, at the start angle ( $A$ )= $0^\circ$ , and  $Da$  and  $Re$  measurements were completed by touching 10 points at  $36^\circ$  angled intervals (Fig. 2). Then, for the same hole, a point on the hole surface at the starting angle  $A=15^\circ$  and  $A=30^\circ$  was touched, and 10 points were touched at  $36^\circ$  angled intervals to measure the hole diameter (dimensional accuracy) and roundness error (Fig. 2). Therefore, 6 measurements were made on the Ti6Al4V component at 1.5 mm and 3 mm depth from the reference surface, and six were made on the CFRP component at 6.5 mm and 8

mm deep. The  $Da_{dev}$  value of that hole was found by subtracting the drill diameter (nominal diameter) from the measured hole diameter value for each hole.  $Da_{dev}$  and  $Re$  values were determined for Ti6Al4V and CFRP by taking the arithmetic average of 6 measurement results for each Ti6Al4V and CFRP component.  $Da$  and  $Re$  measurements of the drilled holes were performed on a UNIVERSAL 10.10 brand 3D Coordinate Measurement Machine (CMM), as seen in Fig. 3.a-c. Ti6Al4V/CFRP metallic stack workpiece material is fixed to the table of the CMM machine by being supported from its side surfaces (Fig. 3).

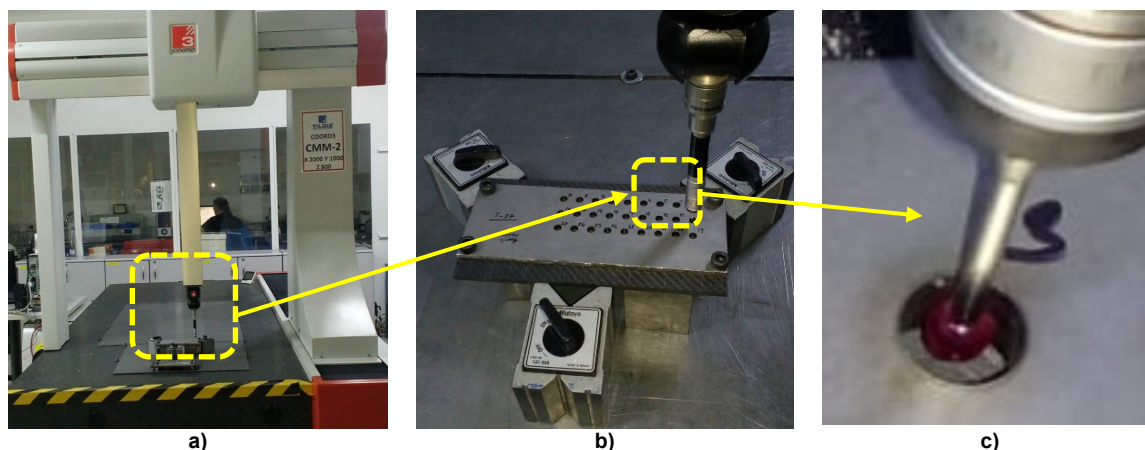


**Figure 3. Dimensional accuracy and roundness error measurements: a) Overview of roundness error and dimensional accuracy measurements on the CMM machine, b) Fixture of the experimental workpiece on the CMM machine, c) Movements of the contact probe in the hole.**

### 2.3. Machining Parameters, Experimental Design, and Multi-Objective Optimization

The levels of the process parameters given in Table 2 were determined by considering the preliminary experiments on the workpiece, the recommendations of the cutting tool company, the performances of the cutting tool-machine tool, and the drilling processes. Since Ti6Al4V alloys have low thermal conductivity, high hardness, and complex chip formation processes compared to CFRP, lower cutting speed and feed rate values were chosen especially considering the Ti alloy [4, 16].

**Table 2. Process parameters and their levels.**

Process Parameters	Unit	Level 1	Level 2	Level 3
Cutting Tool Geometry, ( $T_g$ )	-	8524-100HF (T1 coded)	2475-100F (T2 coded)	5514-RT100U (T3 coded)
Cutting Speed, ( $V_c$ )	m/min	15	21	29
Feed Rate, ( $f$ )	mm/rev	0.040	0.056	0.0784

Taguchi Method was used to determine the effects of process parameters on the surface roughness, dimensional accuracy deviation, and roundness error of the holes in CFRP and Ti6Al4V components in the drilling of CFRP/Ti6Al4V mixed metallic stack because it reduces the experimental study costs and offers a systematic approach, and  $L_{27}(3^3)$  was chosen as the orthogonal array [4]. Since  $Ra$ ,  $Da_{dev}$ , and  $Re$  values

were desired to be the lowest, Taguchi Method evaluations of dependent variables (responses) were made according to the "Smaller is better" approach [4, 5].

Additive Ratio Assessment (ARAS) is one of the multi-criteria decision-making methods [36, 37]. The best alternative is selected based on many attributes using the ARAS method. The final ranking of the alternatives is determined by each alternative's degree of benefit. The ARAS method is based on quantitative measurements and utility theory. The utility function value determines the relative efficiency of an alternative relative to other alternatives [36, 37]. In the ARAS method, qualitative attributes are converted into quantitative attributes, and the attributes are independent. In order to minimize  $Ra$ ,  $Da_{dev}$ , and  $Re$  in both CFRP and Ti6Al4V components, all the steps of the ARAS method were applied respectively when drilling CFRP/Ti6Al4V mixed metallic stack with coated carbide drills. The steps of this method are presented below respectively:

**Step 1. Creating the decision matrix:** The first step of the ARAS method is to create the decision matrix, in which the scores of the alternatives are shown after the alternatives belonging to the decision problem and the criteria to be used to evaluate the alternatives are determined. In the ARAS method, there is a row consisting of the optimal values of each criterion in the initial decision matrix [32-38]. The decision matrix  $X$ , where " $m$ " is the number of alternatives and " $n$ " is the number of criteria, is expressed as shown in Eq. 1.

$$X = \begin{bmatrix} x_{01} & \cdots & x_{0j} & \cdots & x_{0n} \\ \vdots & \ddots & \vdots & \ddots & \vdots \\ x_{i1} & \cdots & x_{ij} & \cdots & x_{in} \\ \vdots & \ddots & \vdots & \ddots & \vdots \\ x_{m1} & \cdots & x_{mj} & \cdots & x_{mn} \end{bmatrix} \quad (1)$$

$$i = 0.1, \dots, m \quad j = 0.1, \dots, n$$

This equation  $x_{ij}$  represents the performance value of the  $i$ th alternative in the  $j$ th criterion and  $x_{0j}$  the optimal value of the  $j$ th criterion [38].

Suppose the optimal value of the criterion is not known in the decision problem. In that case, the optimal value is calculated using Eq. 2 and Eq. 3, respectively, depending on whether the criterion shows benefit (higher is better) or cost (lower is better) [38].

$$x_{0j} = \max_i x_{ij} \quad (2)$$

$$x_{0j} = \min_i x_{ij} \quad (3)$$

**Step 2. Normalization Process and Creating the Normalized Decision Matrix:** "Normalization" is a conversion process that allows the data to be drawn into smaller ranges in cases where the criteria performance values take extensive ranges [38]. In the ARAS method, the normalized decision matrix consists of  $\bar{x}_{ij}$  values. The  $\bar{x}_{ij}$  values are calculated according to whether the criterion shows utility or cost characteristics. If the higher the criterion performance values are considered better (utility), the normalized values are calculated by Eq. 4 [38].

$$\bar{x}_{ij} = \frac{x_{ij}}{\sum_{i=0}^n x_{ij}} \quad (4)$$

If lower criteria performance values are considered better (cost case), the normalization process is performed in two steps. First, the performance values are converted to the utility using Eq. 5; the normalized value is calculated using Eq. 6 [38].

$$x_{ij}^* = \frac{1}{x_{ij}} \quad (5)$$

$$\bar{x}_{ij} = \frac{x_{ij}^*}{\sum_{i=0}^m x_{ij}^*} \quad (6)$$

After calculating the normalized values, the  $\bar{X}$  normalized decision matrix shown in Eq. 7 is obtained [38].

$$\bar{X} = \begin{bmatrix} \bar{x}_{01} & \cdots & \bar{x}_{0j} & \cdots & \bar{x}_{0n} \\ \vdots & \ddots & \vdots & \ddots & \vdots \\ \bar{x}_{i1} & \cdots & \bar{x}_{ij} & \cdots & \bar{x}_{in} \\ \vdots & \ddots & \vdots & \ddots & \vdots \\ \bar{x}_{m1} & \cdots & \bar{x}_{mj} & \cdots & \bar{x}_{mn} \end{bmatrix} \quad (7)$$

$$i = 0.1, \dots, m \quad j = 0.1, \dots, n$$

**Step 3. Creating the Weighted Normalized Decision Matrix:** After the normalized decision matrix is

obtained, the  $\hat{X}$  weighted normalized decision matrix is created using the  $w_j$  criterion importance levels (weights). The weight values of the criteria meet the condition  $0 < w_j < 1$ , and the sum of the weights must be at most 1. Using the normalized values with Eq. 8,  $\hat{x}_{ij}$  weighted normalized values are obtained [38]. In this study, the weights ( $w_j$ ) were determined by dividing the sum of the differences in the S/N response table created for each answer by the Taguchi Method by the sum of the differences of all the answers.

$$\hat{x}_{ij} = \bar{x}_{ij} w_{ij} \quad (8)$$

With the calculated  $\hat{x}_{ij}$  weighted normalized values, the  $\hat{X}$  weighted normalized decision matrix in matrix form is obtained (Eq. 9).

$$\hat{X} = \begin{bmatrix} \hat{x}_{01} & \cdots & \hat{x}_{0j} & \cdots & \hat{x}_{0n} \\ \vdots & \ddots & \vdots & \ddots & \vdots \\ \hat{x}_{i1} & \cdots & \hat{x}_{ij} & \cdots & \hat{x}_{in} \\ \vdots & \ddots & \vdots & \ddots & \vdots \\ \hat{x}_{m1} & \cdots & \hat{x}_{mj} & \cdots & \hat{x}_{mn} \end{bmatrix} \quad (9)$$

$$i = 0.1, \dots, m \quad j = 0.1, \dots, n$$

**Step 4. Calculation of Optimality Function Values:** In the last step of the ARAS method, the optimality function value is calculated for each alternative, and the alternatives are evaluated. The scores of the alternatives are obtained by using Eq. 10 to show the optimality function value ( $S_i$ ) of the  $i$ th choice [38].

$$S_i = \sum_{j=1}^n \hat{x}_{ij} \quad i = 0.1, \dots, m \quad (10)$$

Values larger than the calculated  $s_i$  values indicate more efficient alternatives. Using Eq. 11, the  $s_i$  values of the alternatives are proportional to the  $s_0$  optimal function value, and the  $K_i$  utility degrees are calculated [38].

$$K_i = \frac{s_i}{s_0} \quad i = 0.1, \dots, m \quad (11)$$

The relative efficiency of the utility function values of the alternatives can be calculated by using the  $K_i$  ratios that take values in the range of 0-1. Thus, the values are ordered from largest to smallest, and the alternatives are evaluated [38].

### 3. RESULTS AND DISCUSSION

The surface roughness ( $Ra_{Ti6Al4V}$ ,  $Ra_{CFRP}$ ), deviation from dimensional accuracy ( $Da_{dev\_Ti6Al4V}$ ,  $Da_{dev\_CFRP}$ ), and hole roundness error results ( $Re_{Ti6Al4V}$ ,  $Re_{CFRP}$ ) measured on the hole surfaces of the CFRP composite, and Ti6Al4V alloy in the machinability tests conducted for the evaluation of the drillability of CFRP/Ti6Al4V mixed metallic stacks with coated carbide tools and the optimization of the drilling parameters depending on the cutting tool geometry ( $Tg$ ) and drilling parameters ( $Vc$  and  $f$ ) are presented in Table 3. In Table 3, the results for each response are presented as the arithmetic mean of the

repeated experimental measurement results. This table also presents the S/N ratios (dB) calculated according to the Taguchi method “smaller is the better” criterion.

### 3.1 Effects of Process Parameters on Responses

#### Surface Roughness ( $R_a$ )

This experimental study on the evaluation of machinability of CFRP/Ti6Al4V mixed metallic stacks with cutting tools with different tool geometries it is aimed to determine the optimum drilling parameters in order to obtain minimum surface roughness in both components in one-through drilling of this metallic stack since CFRP, and Ti6Al4V Ti alloy has different mechanical physical and machinability properties. The surface roughness values ( $R_a_{Ti6Al4V}$  and  $R_a_{CFRP}$ ) were measured on the hole surfaces of Ti6Al4V alloy and CFRP composite after drilling the CFRP/Ti6Al4V stack with different geometry cutting tools are presented in Table 3, together with the S/N ratios calculated by the Taguchi Method. It is understood from Table 3 that the average surface roughness measured in CFRP is higher than the average surface roughness measured in Ti6Al4V alloy. While drilling holes in the CFRP

/Ti6Al4V stack with 6.00 mm diameter drills with different geometry,  $R_a$  values were measured in the range of 0.472-1.189  $\mu\text{m}$  for Ti6Al4V Ti alloy, while  $R_a$  values were measured in the range of 2.603-8.318  $\mu\text{m}$  for CFRP composite. Average surface roughness values of 0.751 $\mu\text{m}$  (S/N ratio 2.743dB) and 5.560  $\mu\text{m}$  (S/N ratio -14.497B) were obtained for  $R_a_{Ti6Al4V}$  and  $R_a_{CFRP}$ , respectively. In the drilling of CFRP, the surface roughness of the holes was found to be 641.67% larger on average than the Ti6Al4V alloy. In the study conducted by Isbilir and Ghassemieh,  $R_a$  values in the range of 1.8 $\mu\text{m}$ -6.3 $\mu\text{m}$  on the hole surfaces of the CFRP component and  $R_a$  values in the range of 1.1 $\mu\text{m}$ -3.1 $\mu\text{m}$  on the hole surfaces of the Ti6Al4V component were obtained when drilling CFRP/Ti6Al4V stacks with coated carbide tools with a 140° tip angle. Considering these values, the  $R_a$  values of CFRP are many times higher than Ti6Al4V [13]. In the same study,  $R_a$  values increased with increasing feed rate for CFRP and Ti6Al4V components, while  $R_a$  values decreased with increasing cutting speed.

The feed rate was more effective than the cutting speed [13]. In this context, the results of this study are similar to the results of Isbilir and Ghassemieh.

Table 3. Experimental results and S/N ratios of experimental results

Exp. No	Proses parameters			Experimental results						S/N ratios of experimental results (dB)					
	$T_g$	$V_c$ (m/min)	$f$ (mm/rev)	$Ra_{Ti6Al4V}$ ( $\mu\text{m}$ )	$Ra_{CFRP}$ ( $\mu\text{m}$ )	$Da_{dev\_Ti6Al4V}$ (mm)	$Da_{dev\_CFRP}$ (mm)	$Re_{Ti6Al4V}$ (mm)	$Re_{CFRP}$ (mm)	$Ra_{Ti6Al4V}$	$Ra_{CFRP}$	$Da_{dev\_Ti6Al4V}$	$Da_{dev\_CFRP}$	$Re_{Ti6Al4V}$	$Re_{CFRP}$
1	T1 (8524-100HF)	15	0.040	0.589	4.753	0.033729	0.543538	0.010341	0.060418	4.60	-13.54	29.44	5.30	39.71	24.38
2	T1 (8524-100HF)	15	0.056	0.737	8.224	0.042375	0.836571	0.005783	0.079976	2.65	-18.30	27.46	1.55	44.76	21.94
3	T1 (8524-100HF)	15	0.078	1.189	8.318	0.048054	0.918660	0.006629	0.076828	-1.51	-18.40	26.37	0.74	43.57	22.29
4	T1 (8524-100HF)	21	0.040	0.667	5.913	0.037647	0.557697	0.006992	0.048471	3.52	-15.44	28.49	5.07	43.11	26.29
5	T1 (8524-100HF)	21	0.056	0.963	6.719	0.043540	0.699366	0.010060	0.112978	0.33	-16.55	27.22	3.11	39.95	18.94
6	T1 (8524-100HF)	21	0.078	0.643	7.226	0.044306	1.314353	0.005761	0.088776	3.83	-17.18	27.07	-2.37	44.79	21.03
7	T1 (8524-100HF)	29	0.040	0.472	6.301	0.027366	0.458773	0.008270	0.122390	6.51	-15.99	31.26	6.77	41.65	18.25
8	T1 (8524-100HF)	29	0.056	0.510	5.681	0.034634	1.073797	0.007674	0.162233	5.86	-15.09	29.21	-0.62	42.30	15.80
9	T1 (8524-100HF)	29	0.078	0.682	4.677	0.033614	0.638347	0.007610	0.072590	3.32	-13.40	29.47	3.90	42.37	22.78
10	T2 (2475-100F)	15	0.040	0.752	2.727	0.029607	0.627944	0.009564	0.040799	2.48	-8.71	30.57	4.04	40.39	27.79
11	T2 (2475-100F)	15	0.056	0.911	5.942	0.029979	0.970412	0.006886	0.087920	0.81	-15.48	30.46	0.26	43.24	21.12
12	T2 (2475-100F)	15	0.078	1.069	7.459	0.031978	0.938320	0.007795	0.091309	-0.58	-17.45	29.90	0.55	42.16	20.79
13	T2 (2475-100F)	21	0.040	0.666	6.023	0.027588	1.159459	0.007060	0.093676	3.53	-15.60	31.19	-1.29	43.02	20.57
14	T2 (2475-100F)	21	0.056	0.956	6.119	0.032724	0.911425	0.008315	0.078876	0.39	-15.73	29.70	0.81	41.60	22.06
15	T2 (2475-100F)	21	0.078	0.692	6.420	0.034379	0.780356	0.008902	0.072517	3.20	-16.15	29.27	2.15	41.01	22.79
16	T2 (2475-100F)	29	0.040	0.583	2.644	0.032521	0.690457	0.006901	0.056742	4.69	-8.45	29.76	3.22	43.22	24.92
17	T2 (2475-100F)	29	0.056	0.701	4.740	0.034500	0.844879	0.007732	0.066847	3.08	-13.52	29.24	1.46	42.23	23.50
18	T2 (2475-100F)	29	0.078	0.660	5.689	0.033522	0.349956	0.009179	0.047783	3.61	-15.10	29.49	9.12	40.74	26.41
19	T3 (5514-RT100U)	15	0.040	0.712	2.603	0.033095	0.726113	0.008960	0.045490	2.95	-8.31	29.60	2.78	40.95	26.84
20	T3 (5514-RT100U)	15	0.056	0.788	6.733	0.034691	0.651348	0.007046	0.083833	2.07	-16.56	29.20	3.72	43.04	21.53
21	T3 (5514-RT100U)	15	0.078	0.979	4.491	0.034335	0.441052	0.007404	0.060762	0.18	-13.05	29.29	7.11	42.61	24.33
22	T3 (5514-RT100U)	21	0.040	0.475	5.095	0.142162	0.399294	0.007641	0.084705	6.47	-14.14	16.94	7.97	42.34	21.44
23	T3 (5514-RT100U)	21	0.056	0.821	4.256	0.119431	1.093333	0.006459	0.067135	1.71	-12.58	18.46	-0.78	43.80	23.46
24	T3 (5514-RT100U)	21	0.078	0.956	3.172	0.130625	0.136017	0.010110	0.023740	0.39	-10.03	17.68	17.33	39.91	32.49
25	T3 (5514-RT100U)	29	0.040	0.515	5.186	0.046752	0.733125	0.011607	0.071670	5.77	-14.30	26.60	2.70	38.71	22.89
26	T3 (5514-RT100U)	29	0.056	0.734	5.671	0.055518	1.159950	0.011564	0.075440	2.69	-15.07	25.11	-1.29	38.74	22.45
27	T3 (5514-RT100U)	29	0.078	0.842	7.337	0.050308	0.575192	0.012455	0.071858	1.49	-17.31	25.97	4.80	38.09	22.87
	Maximum			1.189	8.318	0.142162	1.314353	0.012455	0.162233						
	Minimum			0.472	2.603	0.027366	0.136017	0.005761	0.023740						
	Mean			0.751	5.560	0.047370	0.749249	0.008322	0.075769						

The higher  $Ra$  surface roughness values measured in CFRP are generally attributed to the uncut fibers and the brittle nature of the fibers that are deformed and cut due to brittle fracture during drilling. On the other hand, tool wear and thrust forces also cause an increase in surface roughness values. Low and high cutting speeds cause fiber breaks, shrinkage, and cracks on the hole surface. When drilling CFRP, the surface roughness is also affected by the low-temperature strength of the matrix, which is typically below 180°C. Temperatures higher than 180°C results in material softening, material degradation, and poor surface quality [2]. According to Kim et al., hole circularity and surface roughness trends are very similar in CFRP holes of the stack. According to the researchers, carbon fiber pull-out affects the hole roundness of CFRP and the surface roughness. Carbon fiber pull-out is a type of machined CFRP surface defect caused by the removal of carbon fiber bundles, mostly in micron size when they are pulled away by fiber-matrix debonding and matrix stripping [12]. Although there are many reasons for the relatively greater surface roughness of the drilled CFRP surface, fiber pull-out is the main cause. When carbon fiber bundles are removed during drilling, the machined surface becomes rough, and the hole profile deviates further [12]. On the other hand, unlike the CFRP layers, the average surface roughness values of the Ti layer remain relatively more consistent [8, 10, 12, 18, 24, 39, 40].

The  $Ra$  surface roughnesses obtained when drilling the CFRP composite depending on the cutting tool geometry are evaluated; T3 (5514-RT100U) coded tools provided the lowest  $Ra$  values. When the  $Ra$  surface roughnesses obtained in drilling the Ti6Al4V alloy depending on the cutting tool geometry are evaluated, T1 (8524-100HF) coded tools provided the lowest  $Ra$  values. Compared to the T1 coded tool, the average  $Ra$  values measured in drilling with the T3 (5514-RT100U) and T2 (2475-100F) coded tools were higher by 5.72% and 8.37%, respectively, compared to the T1 tool. Compared to the T3 coded tool, the average  $Ra$  values measured in drilling with the T2 (2475-100F) and T1 (8524-100HF) coded tools were higher by 7.23% and 29.80%, respectively, compared to the T3 tool.

The mean  $Ra_{Ti6Al4V}$  values, the mean S/N ratio values for the mean  $Ra_{Ti6Al4V}$  values, the mean  $Ra_{CFRP}$  values, and the mean S/N ratio values for the

mean  $Ra_{CFRP}$  values at different levels of the control factors are presented in Table 4. The S/N ratio analysis gave important information about the roughness of the hole surfaces of the Ti6Al4V and CFRP components when drilling CFRP/Ti6Al4V mixed metallic stack with different geometry carbide drills under the selected conditions. The higher or lower differences between the S/N ratio values calculated at different levels of each control factor were used to determine the effective factors on  $Ra_{Ti6Al4V}$  and  $Ra_{CFRP}$ . Since the roughness of the hole surfaces is desired to be the lowest in drilling, the lowest  $Ra$  values at different levels of the control factors have been taken into account. As indicated by "\*" in Table 4; the optimum levels of control factors for  $Ra_{Ti6Al4V}$  were determined as  $Tg1Vc3f1$  ( $Tg=T1(8524-100HF)$  coded tool,  $Vc=29$  m/min,  $f=0.040$  mm/rev). The most effective parameters on  $Ra_{Ti6Al4V}$  with values of 0.2535 $\mu$ m (2.952dB), 0.2253 $\mu$ m (2.597dB) and 0.0598 $\mu$ m (0.879dB) were determined as feed rate, cutting speed and cutting tool geometry, respectively (Table 4). The optimum levels of control factors for  $Ra_{CFRP}$  were determined as  $Tg3Vc3f1$  ( $Tg=T3(5514-RT100U)$  coded set,  $Vc=29$  m/min,  $f=0.040$  mm/rev). The most effective parameters on  $Ra_{CFRP}$  with values of 1.505 $\mu$ m (2.71dB), 1.474 $\mu$ m (2.500dB) and 0.369 $\mu$ m (0.57dB) were determined as feed rate, cutting tool geometry and cutting speed, respectively (Table 3). In the study of Isbilir and Ghassemieh, the feed rate was more effective than the cutting speed [13]. The main effect graphs showing the effects of control factors on  $Ra_{Ti6Al4V}$  and  $Ra_{CFRP}$  are presented in Fig. 4. As can be seen in Fig. 4.a, optimum levels of control factors for the hole surface roughness  $Ra_{Ti6Al4V}$  of Ti6Al4V Ti alloy when drilling CFRP/Ti6Al4V metallic stack with different geometry drills,  $Tg1Vc3f1$  ( $Tg=T1(8524-100HF)$  coded tool,  $Vc=29$  m/min,  $f=0.040$  mm/rev).

It is seen in Fig. 4.b that the optimum levels for  $Ra_{CFRP}$  are  $Tg3Vc3f1$  ( $Tg=T3(5514-RT100U)$  coded tool,  $Vc=29$  m/min,  $f=0.040$  mm/rev). While lower  $Ra$  surface roughness values were obtained when drilling Ti6Al4V alloy with T1 coded tool, the lowest  $Ra$  roughness values were obtained with T3 coded tool when drilling CFRP.

**Table 4. Response table for Means and Signal to Noise Ratios of  $Ra_{Ti6Al4V}$  and  $Ra_{CFRP}$ .**

Responses for Means				Responses for S/N Ratios			
$Ra_{Ti6Al4V}$ ( $\mu$ m)				S/N ratio for $Ra_{Ti6Al4V}$ (dB)			
Level	$Tg$	$Vc$	$f$	Level	$Tg$	$Vc$	$f$
1	0.7169*	0.8585	0.6034*	1	3.236*	1.516	4.502*
2	0.7766	0.7598	0.7912	2	2.357	2.598	2.176
3	0.758	0.6332*	0.8569	3	2.635	4.113*	1.55
Difference	0.0598	0.2253	0.2535	Difference	0.879	2.597	2.952
Rank	3	2	1	Rank	3	2	1
$Ra_{CFRP}$ ( $\mu$ m)				S/N ratio for $Ra_{CFRP}$ (dB)			
Level	$Tg$	$Vc$	$f$	Level	$Tg$	$Vc$	$f$
1	6.423	5.694	4.583*	1	-15.99	-14.42	-12.72*
2	5.307	5.66	6.009	2	-14.02	-14.82	-15.43
3	4.949*	5.325*	6.087	3	-13.48*	-14.25*	-15.34
Difference	1.474	0.369	1.505	Difference	2.5	0.57	2.71
Rank	2	3	1	Rank	2	3	1

(\*) Optimum level

The lower  $R_a$  value obtained when drilling Ti6Al4V alloy with T1 coded tool is attributed to the nano-Si coating layer, slightly concave main cutting edge, body thinning value, and lightened cone form of this drill. Nano-Si coating provides high resistance to tool wear. Due to the concave form, chip formation and impossibility are facilitated in cutting Ti alloy with a low machinability ratio, and corner wear is reduced. While drilling a hole through the metallic stack in one go, the surface roughness values decreased with the increase of the cutting speed, valid for each component, while the surface roughness values increased with the increase of the feed rate [13].

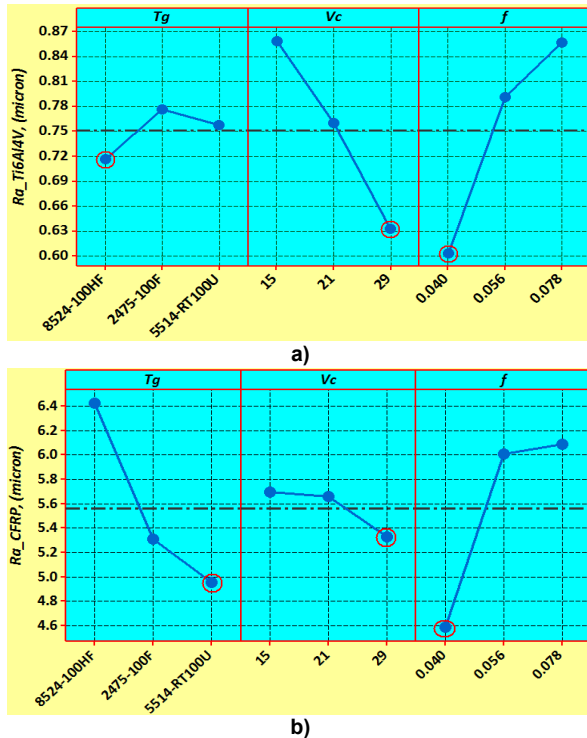


Figure 4. Main effect plot for  $R_a_{Ti6Al4V}$  and  $R_a_{CFRP}$ : a)  $R_a_{Ti6Al4V}$ , b)  $R_a_{CFRP}$

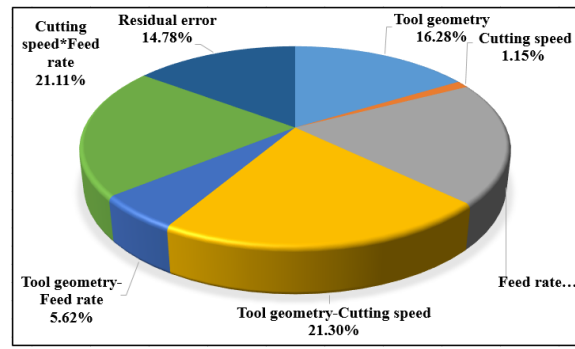
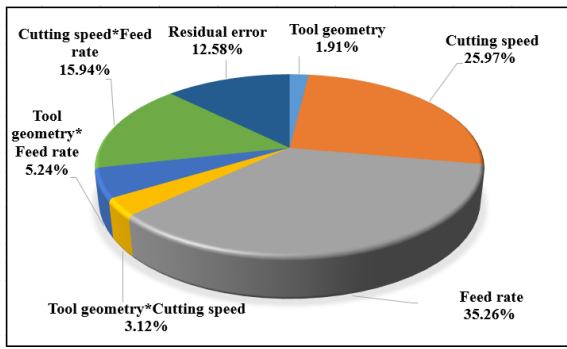
Ti and Ti alloys are in the difficult-to-cut material group. In general, with the increase in cutting speed, the volume of chips on the cutting edge will increase. Due to intensified heat transfer and temperature rise, the tool's cutting edge will wear (or lose its sharpness), and its ability to make clean cuts will decrease. As a result, the roughness values of the hole surfaces will increase. The reason why lower  $R_a$  values were obtained in Ti6Al4V Ti alloy and CFRP at higher cutting speeds is as follows: First of all, it should be noted that the machinability of CFRP is higher than Ti alloy. In this study, when a stack is drilled through, the total thickness of the drilled hole does not exceed 10 mm, and the chip volume removed is very small since only one hole is drilled.

The heat-generating during cutting, which makes the machinability of the Ti6Al4V Ti alloy lower and inherent deterioration of the CFRP composite structure, was not present in described experiments. Therefore, despite drilling at high cutting speeds, prolonged chip removal does not occur, which causes rapid wear of the tool and a significant reduction in the sharpness of the cutting edge. At a constant feed rate, the cutting edges of the cutting tool will repeatedly touch the surfaces they cut in their previous revolutions due to the higher rotation speed at high cutting speed. As a result, the work material in the form of peaks on the hole surfaces, where the cutting edges of the cutting tool cannot be completely cut in the previous rotation, will also be cut, and a smoother surface will be obtained.  $R_a$  values are also lower for all these reasons since the integrity of the drill cutting edge is preserved at high cutting speeds. The hole surface quality of the Ti6Al4V and CFRP components deteriorated with increasing feed rates. Increasing the surface roughness value is a valid issue for all materials depending on the feed rate. These results show parallelism with the results of studies on similar materials in the literature [8, 10, 13, 18, 24, 39, 40].

Analysis of Variance (ANOVA) at a 95% confidence level was performed to determine the effects of control factors on selected performance/quality characteristics. ANOVA results for  $R_a_{Ti6Al4V}$  and  $R_a_{CFRP}$ , including control factors and interactions of control factors, are presented in Table 5. The most influential factor on  $R_a_{Ti6Al4V}$  was the feed rate, with a 35.26% contribution rate. The feed rate was followed by the cutting speed and the cutting speed-feed rate interaction with 25.97% and 15.94% contribution rates, respectively (Table 5. a) [41]. The most effective parameter on  $R_a_{CFRP}$  was the cutting tool geometry-cutting speed interaction with a 21.30% contribution rate. It was followed by the interaction of cutting speed-feed rate, feed rate, and cutting tool geometry with contribution rates of 21.11%, 19.77%, and 16.28% in terms of % effect (Table 5. b) [41]. The effects of other control factors and factor interactions on  $R_a_{Ti6Al4V}$  and  $R_a_{CFRP}$  remained below 10%.

Table 5. ANOVA results for  $R_a_{Ti6Al4V}$  and  $R_a_{CFRP}$ .

a) $R_a_{Ti6Al4V}$							b) $R_a_{CFRP}$						
Source	Degree of Freedom	Sum of Square	Mean Square	F Table	P	Cont. %	Source	Degree of Freedom	Sum of Square	Mean Square	F Table	P	Cont. %
$T_g$	2	0.01684	0.008418	0.61	0.569	1.91	$T_g$	2	10.6423	5.3211	4.41	0.051	16.28
$V_c$	2	0.22959	0.114794	8.26	0.011	25.97	$V_c$	2	0.7491	0.3746	0.31	0.742	1.15
$f$	2	0.31163	0.155814	11.21	0.005	35.26	$f$	2	12.9194	6.4597	5.35	0.033	19.77
$T_g*V_c$	4	0.02754	0.006884	0.5	0.74	3.12	$T_g*V_c$	4	13.9246	3.4812	2.88	0.095	21.30
$T_g*f$	4	0.04629	0.011573	0.83	0.541	5.24	$T_g*f$	4	3.6735	0.9184	0.76	0.579	5.62
$V_c*f$	4	0.14086	0.035216	2.53	0.123	15.94	$V_c*f$	4	13.796	3.449	2.86	0.096	21.11
Residual Error	8	0.11118	0.013898			12.58	Res. Error	8	9.6579	1.2072			14.78
Total	26	0.88393				100.00	Total	26	65.3628				100.00
S=0.1179 $R^2=87.4\%$ $R^2(\text{adjusted})=59.1\%$							S=1.099 $R^2=85.2\%$ $R^2(\text{adjusted})=52.0\%$						



### Deviation from Dimensional Accuracy ( $Da_{dev}$ )

When drilling CFRP/Ti6Al4V stack with different coated carbide drills, the measured hole diameter values for Ti6Al4V alloy and CFRP composite after machining, deviation values from the nominal hole diameter (drill diameter=6.00mm) ( $Da_{dev\_Ti6Al4V}$  and  $Da_{dev\_CFRP}$ ) values and S/N ratios calculated by Taguchi method are presented in Table 3. It is understood from Table 3 that the mean deviation from dimensional accuracy calculated for CFRP is higher than the mean deviation from dimensional accuracy calculated for Ti6Al4V Ti alloy [7, 8, 10, 18-21, 42]. While drilling holes in the CFRP/Ti6Al4V stack with 6.00 mm diameter drills with different geometry,  $Da_{dev}$  values were measured in 0.0277366-0.047370 mm for Ti6Al4V Ti alloy, while  $Da_{dev}$  values were measured in the range of 0.136017-1.314353 mm for CFRP composite. The mean deviations from dimensional accuracy were obtained for Ti6Al4V and CFRP of 0.047370mm (S/N ratio 27.57dB) and 0.749249mm (S/N ratio 3.26dB), respectively. The deviation values of the dimensional accuracy of the holes in the CFRP drilling were 1481.70% higher on average than the Ti6Al4V alloy [7, 8, 10, 17-21, 24, 42]. The deviation from the dimensional accuracy obtained in the drilling of Ti6Al4V alloy is evaluated depending on the cutting tool geometry; T2 (2475-100F) provided the lowest  $Da_{dev}$  values. The average  $Da_{dev}$  values measured for drilling with tools T1 (8524-100HF) and T3 (5514-RT100U) were 20.39% and 125.57% higher on average, respectively,

compared to the T2 code tool. When the deviation from the dimensional accuracy obtained in the drilling of the CFRP composite depending on the cutting tool geometry is evaluated, the T3 (5514-RT100U) coded tools provided the lowest  $Da_{dev}$  values. The average  $Da_{dev}$  values measured in drilling with T1 (8524-100HF) and T2 (2475-100F) coded tools were 19.03% and 22.95% higher on average, respectively, compared to the T3 tool. The mean  $Da_{dev\_Ti6Al4V}$  values, the mean S/N ratio values for the mean  $Da_{dev\_Ti6Al4V}$  values, the mean  $Da_{dev\_CFRP}$  values, and the mean S/N ratio values for the average  $Da_{dev\_CFRP}$  values measured and then calculated for the experiments performed at different levels of control factors are presented in Table 6. The S/N ratio analysis gave important information about the nature of the deviations of Ti6Al4V and CFRP components from their nominal hole diameters when drilling CFRP/Ti6Al4V metallic stack with different geometry carbide drills under the selected conditions. As indicated by "\*" in Table 6, the optimum levels of control factors for  $Da_{dev\_Ti6Al4V}$  were determined as  $Tg2Vc1f1$  ( $Tg=T2$  (2475-100F) coded tool,  $Vc=15m/min$ ,  $f=0.040mm/rev$ ). The most effective parameters on  $Da_{dev\_Ti6Al4V}$  were determined as cutting tool geometry, cutting speed and feed rate, with values of 0.04001mm (5.64dB), 0.03273mm (4.03dB) and 0.00341mm (1.04dB), respectively (Table 6). The optimum levels of control factors for  $Da_{dev\_CFRP}$  were determined as  $Tg3Vc3f1$  ( $Tg=T3$  (5514-RT100U) coded tool,  $Vc=29m/min$ ,  $f=0.040mm/rev$ ).

Table 6. Response table for Means and Signal to Noise Ratios of  $Da_{dev\_Ti6Al4V}$  and  $Da_{dev\_CFRP}$ .

Responses for Means				Responses for S/N Ratios			
$Da_{dev\_Ti6Al4V}$ (mm)				S/N ratio for $Da_{dev\_Ti6Al4V}$ (dB)			
Level	$Tg$	$Vc$	$f$	Level	$Tg$	$Vc$	$f$
1	0.03836	0.03532*	0.04561*	1	28.44	29.14	28.21
2	0.03187*	0.06804	0.04749	2	29.95	25.11	27.34
3	0.07188	0.03875	0.04901	3	24.32	28.46	27.17
Difference	0.04001	0.03273	0.00341	Difference	5.64	4.03	1.04
Rank	1	2	3	Rank	1	2	3
$Da_{dev\_CFRP}$ (mm)				S/N ratio for $Da_{dev\_CFRP}$ (dB)			
Level	$Tg$	$Vc$	$f$	Level	$Tg$	$Vc$	$f$
1	0.7823	0.7393	0.6552*	1	2.6038	2.8946	4.0622
2	0.8081	0.7835	0.9157	2	2.259	3.5562	0.9142
3	0.6573*	0.7249*	0.6769	3	4.9281	3.3401	4.8145
Difference	0.1509	0.0585	0.2605	Difference	2.669	0.6615	3.9003
Rank	2	3	1	Rank	2	3	1

(\* Optimum level)

The most effective parameters on  $Da_{dev\_CFRP}$  were determined as the feed rate, cutting tool geometry and cutting speed, with values of 0.2605mm (3.9003dB), 0.1509mm (2.669dB) and 0.0585mm (0.6615dB), respectively (Table 6). The main effect graphs indicating the effects of control factors on  $Da_{dev\_Ti6Al4V}$  are presented in Fig. 5.a, and the main effect graphs indicating the effects on  $Da_{dev\_CFRP}$  are presented in Fig. 5.b. As can be seen in Fig. 5.a, the optimum levels of control factors for  $Da_{dev\_Ti6Al4V}$  are  $Tg2Vc1f1$  ( $Tg=T2$  (2475-100F) coded tool,  $Vc=15$ m/min,  $f=0.040$ mm/rev) when drilling CFRP/Ti6Al4V metallic stack with different geometry drills, respectively. Fig. 5.a shows that optimum levels for  $Da_{dev\_CFRP}$  are  $Tg3Vc3f1$  ( $Tg=T3$  (5514-RT100U)) coded tool,  $Vc=29$ m/min,  $f=0.040$ mm/rev). While lower deviation from dimensional accuracy values was obtained in drilling Ti6Al4V alloy with T2 coded tool, the lowest deviation from dimensional accuracy values was obtained with T3 coded tool in drilling CFRP. T3 coded tools also provided lower Ra surface roughness values when drilling CFRP (Subsection 3.1.1). The T3-coded tool outperforms  $Da_{dev\_CFRP}$  compared to other cutting tools due to the factors explained in detail in Subsection 3.2.1. If a special metal drill bit is used to drill CFRP/Ti stack, such a drill bit is usually of stepped construction or has a large tip angle, resulting in excessive thrust force in drilling.

As a result, hole damage in the form of delamination and fiber removal increases CFRP. In addition, although the drill bit with a small tip angle can produce less thrust force than the drill with a large tip angle when drilling the stack, larger torque will occur when drilling the Ti alloy, which can easily cause drill breakage. Of course, the drill should not break in a machining operation. Therefore, this type of drill structure may not be suitable for drilling Ti/CFRP stack, and it is necessary to ensure that the tip angle is designed between  $130^\circ$  and  $140^\circ$  [43]. On the other hand, it is also stated that a drill with a smaller tip angle, shorter sharp edge, and lower helix angle will reduce the thrust force, delamination, and roundness deviation [43]. In the study by Jia, it is stated that the length of the cutting edge, the drill bit angle, and the helix angle play a vital role in CFRP/Ti drilling [1]. The same study states that a stepped drill with a tip angle of  $140^\circ$  can reduce the thrust force in drilling with a higher feed rate. Hole quality also increases with the reduction of the thrust force.

In summary, in studies on drill geometries, it has been seen that tool geometries significantly contribute to improving hole quality, thrust force, roundness, and dimensional accuracy when drilling Ti/CFRP stacks. The drills (T1, T2, and T3 coded drills) used in this experimental study have a tip angle of  $140^\circ$ . In this context, drills with the correct tip angle were selected for this study. While drilling through the metallic stack in one go, lower-dimensional accuracy deviation values were obtained at the lowest cutting speed in Ti6Al4V Ti alloy and at the highest cutting speed in CFRP composite (Fig. 5, Table 6).

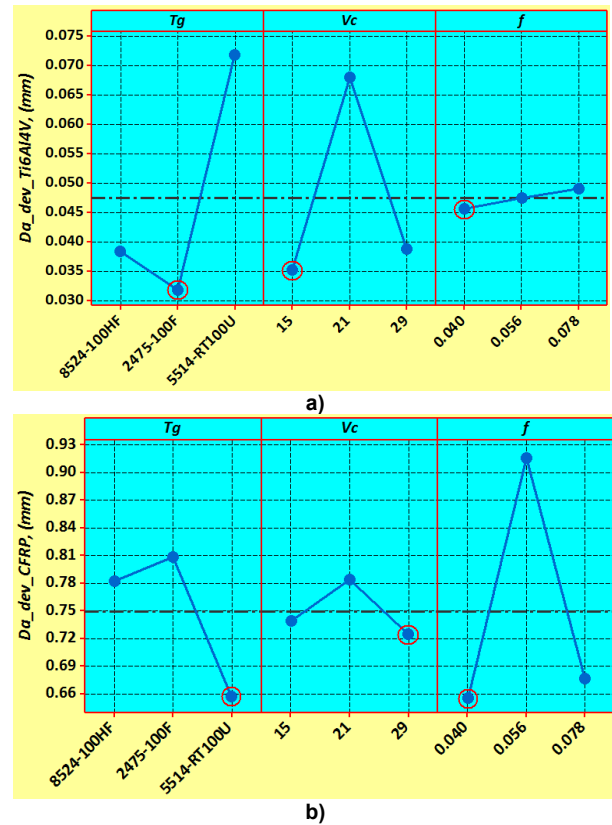


Figure 5. Main effect plot for  $Da_{dev\_Ti6Al4V}$  and  $Da_{dev\_CFRP}$ : a)  $Da_{dev\_Ti6Al4V}$ , b)  $Da_{dev\_CFRP}$

The machinability of Ti alloy is lower than that of CFRP composite. High cutting speeds mean a larger hole diameter for Ti6Al4V Ti alloy, as the drill's main and auxiliary cutting edges lose sharpness, or the micro-size hardened Ti alloy material adhering to the cutting edge repeatedly scratches the hole surfaces at each revolution. The reason for the deviation from lower dimensional accuracy in CFRP composite at higher cutting speed is that the machinability of CFRP is higher than the Ti alloy, and the matrix and the fiber reinforcement elements in the matrix can be easily cut. At the same time, the hole diameter is formed during cutting even at high cutting speeds, and those that cannot be cut can be easily cut from the high cutting speed. This is because it was cut in the next cycles, so a more consistent and higher hole diameter accuracy was obtained. Again, a lower deviation from dimensional accuracy values was obtained for both CFRP, and Ti6Al4V components at low feed rate drilling of CFRP/Ti6Al4V mixed metallic stack [7, 8, 10, 17, 18, 20, 21, 24, 42].

ANOVA results for  $Da_{dev\_Ti6Al4V}$  and  $Da_{dev\_CFRP}$ , including the effects of control factors and their interactions, are presented in Table 7. The most influential factor on  $Da_{dev\_Ti6Al4V}$  was the cutting tool geometry-cutting speed interaction ( $Tg*Vc$ ) with a 41.56% contribution rate. The cutting tool geometry-cutting speed interaction followed the cutting tool geometry and cutting speed, with contribution ratios of 33.19% and 23.29%, respectively (Table 7. a). No statistically significant effect of feed rate on  $Da_{dev\_Ti6Al4V}$  was detected. The most effective parameter on  $Da_{dev\_CFRP}$  was the cutting tool

geometry-feed rate ( $Tg*f$ ) interaction with a 26.48% contribution rate. The cutting tool geometry-feed rate interaction followed feed rate and cutting tool geometry-cutting speed ( $Tg*Vc$ ) interaction with 18.55% and 14.91% contribution rates, respectively (Table 7. b). The effects of other control factors and factor interactions on  $Da_{dev\_Ti6Al4V}$  and  $Da_{dev\_CFRP}$  were insignificant.

### 3.2 Roundness Error (Re)

Hole roundness error values ( $Re_{Ti6Al4V}$  and  $Re_{CFRP}$ ) measured after machining for Ti6Al4V alloy and CFRP composite when drilling CFRP/Ti6Al4V stack with coated carbide drills are presented in Table 3, together with the S/N ratios calculated by the Taguchi method. It is understood from Table 3 that the mean of roundness error of the holes drilled in CFRP is higher than the mean of roundness error measured in Ti6Al4V Ti alloy [7, 8,

10, 18, 20, 21, 24, 42]. While drilling holes in the CFRP/Ti6Al4V stack with 6.00 mm diameter drills with different geometry,  $Re$  values, were measured in the range of 0.005761-0.012455mm for Ti6Al4V Ti alloy, while  $Re$  values were measured in the range of 0.023740-0.162233mm for CFRP composite. Average  $Re$  roundness error values of 0.008322mm (S/N ratio 41.78dB) and 0.075769mm (S/N ratio 22.96dB) were obtained for  $Re_{Ti6Al4V}$  and  $Re_{CFRP}$ , respectively. In the drilling of CFRP, the roundness error values of the holes  $Re$  were 810.47% larger on average than the Ti6Al4V alloy [6-9, 17, 19, 20, 23, 38]. The reasons for the occurrence of larger hole roundness error in CFRP are as follows: (1) Deformation of the matrix on the hole surface due to the short-term heat effect that may occur with fiber separations and stripping on the hole surface during the drilling of CFRP, (2) During the cutting of the Ti alloy component, hard and

Table 7. ANOVA results for  $Da_{dev\_Ti6Al4V}$  and  $Da_{dev\_CFRP}$ .

a) $Da_{dev\_Ti6Al4V}$						b) $Da_{dev\_CFRP}$							
Source	Degree of Freedom	Sum of Square	Mean Square	F Table	P	Cont. %	Source	Degree of Freedom	Sum of Square	Mean Square	F Table	P	Cont. %
$Tg$	2	0.0083	0.00415	154.33	0.000*	33.19	$Tg$	2	0.11721	0.058604	0.92	0.436	5.78
$Vc$	2	0.005824	0.002912	108.29	0.000*	23.29	$Vc$	2	0.01675	0.008374	0.13	0.878	0.83
$f$	2	0.000052	0.000026	0.97	0.418	0.21	$f$	2	0.37605	0.188025	2.96	0.109	18.55
$Tg*Vc$	4	0.010394	0.002599	96.64	0.000*	41.56	$Tg*Vc$	4	0.30221	0.075552	1.19	0.386	14.91
$Tg*f$	4	0.00013	0.000033	1.21	0.378	0.52	$Tg*f$	4	0.53689	0.134222	2.11	0.171	26.48
$Vc*f$	4	0.000093	0.000023	0.86	0.525	0.37	$Vc*f$	4	0.16966	0.042414	0.67	0.633	8.37
Residual Error	8	0.000215	0.000027			0.86	Residual Error	8	0.50862	0.063578			25.09
Total	26	0.025009				100.00	Total	26	2.02738				100.00

S=0.005186  $R^2=99.1\%$   $R^2(\text{adjusted})=97.2\%$       S=0.2521  $R^2=74.9\%$   $R^2(\text{adjusted})=18.5\%$   
 (\*) Statistically significant parameter (P<0.05)

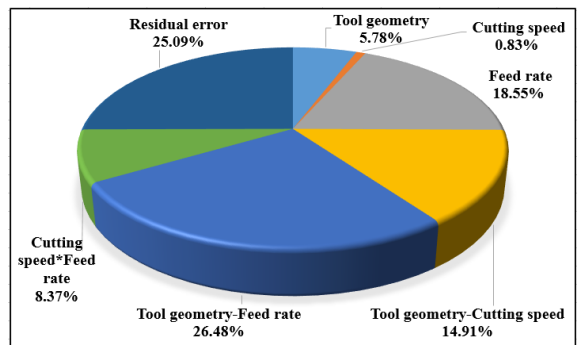
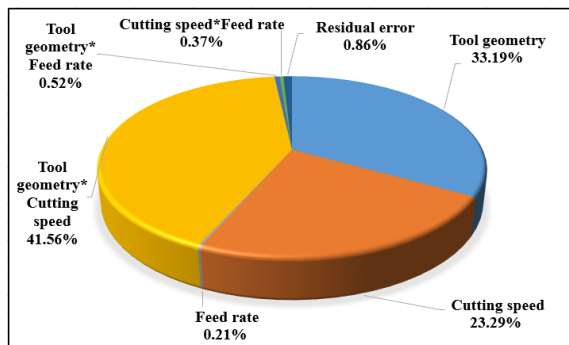


Table 8. Response table for Means and Signal to Noise Ratios of  $Re_{Ti6Al4V}$  ve  $Re_{CFRP}$ .

Responses for Means				Responses for S/N Ratios			
$Re_{Ti6Al4V}$ (mm)				S/N ratio for $Re_{Ti6Al4V}$ (dB)			
Level	$Tg$	$Vc$	$f$	Level	$Tg$	$Vc$	$f$
1	0.00768*	0.007823*	0.008593	1	42.47	42.27	41.46
2	0.008037	0.007922	0.007946*	2	41.96	42.17	42.18
3	0.009249	0.009221	0.008427	3	40.91	40.9	41.7
Difference	0.001569	0.001398	0.000646	Difference	1.56	1.38	0.73
Rank	1	2	3	Rank	1	2	3
$Re_{CFRP}$ (mm)				S/N ratio for $Re_{CFRP}$ (dB)			
Level	$Tg$	$Vc$	$f$	Level	$Tg$	$Vc$	$f$
1	0.09163	0.0697*	0.06937	1	21.3	23.44	23.71
2	0.07072	0.07454	0.09058	2	23.33	23.23	21.2
3	0.06496*	0.08306	0.06735*	3	24.26	22.21	23.98
Difference	0.02667	0.01336	0.02323	Difference	2.96	1.24	2.78
Rank	1	3	2	Rank	1	3	2

(\*) Optimum level

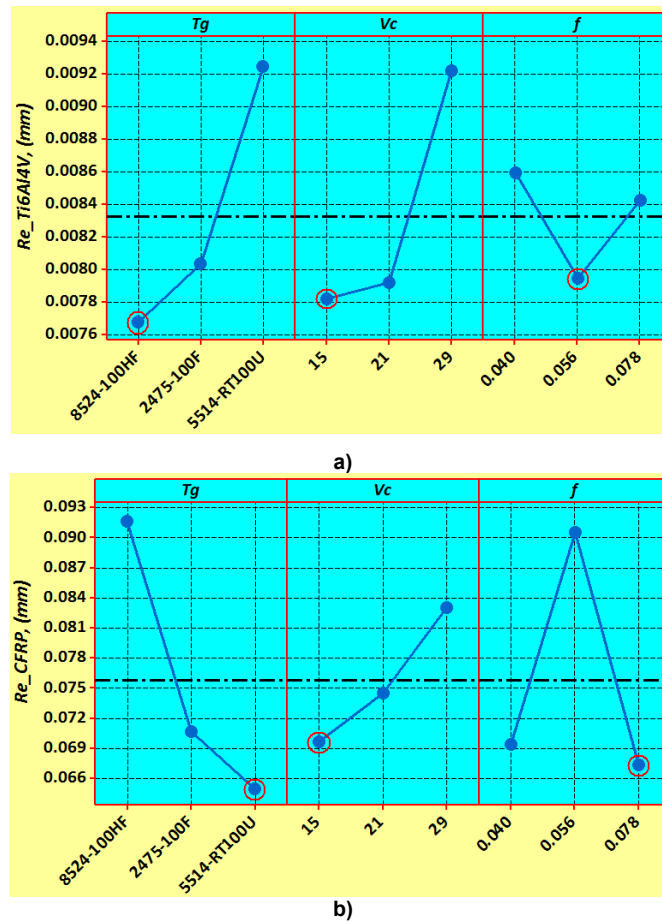


Figure 5. Main effect plot for  $Da_{dev\_Ti6Al4V}$  and  $Da_{dev\_CFRP}$ : a)  $Da_{dev\_Ti6Al4V}$ , b)  $Da_{dev\_CFRP}$

the sharp chips of Ti alloy destroy the hole surfaces of the CFRP during the outward movement of the drill flutes. When the  $Re$  roundness error values obtained in drilling the Ti6Al4V alloy depending on the cutting tool geometry are evaluated, T1 (8524-100HF) coded tools provided the lowest  $Re$  values. Compared to the T1 coded tool, the average  $Re$  values measured in drilling with the T2 (2475-100F) and T3 (5514-RT100U) tools were higher by 4.65% and 20.44%, respectively. Considering the roundness error obtained in the drilling of CFRP composite depending on the cutting tool geometry, T3 (5514-RT100U) coded tools provided the lowest  $Re$  values. Compared to the T3 coded tool, the average  $Re$  values measured in drilling with the T2 (2475-100F) and T1 (8524-100HF) coded tools were 8.87% and 41.06% higher, respectively, compared to the T3 tool. The mean  $Re_{Ti6Al4V}$  values, the average S/N ratio values for the mean  $Re_{Ti6Al4V}$  values, the mean  $Re_{CFRP}$  values, and the mean S/N ratio values for the mean  $Re_{CFRP}$  values of the drilled holes in the experiments performed at different levels of control factors are presented in Table 8. As indicated by "\*" in Table 8; Optimum levels of control factors for  $Re_{Ti6Al4V}$  were determined as  $Tg1Vc1f2$  (T1 (8524-100HF) coded tool,  $Vc=15$  m/min,  $f=0.056$  mm/rev). The most effective parameters on  $Re_{Ti6Al4V}$  were determined as cutting tool geometry, cutting speed and feed rate, with values of 0.001569mm (1.56dB), 0.001398mm (1.38dB) and 0.000646mm (0.73dB), respectively (Table 7). As indicated by "\*" in Table 8; Optimum levels of control

factors for  $Re_{Ti6Al4V}$  were determined as  $Tg1Vc1f2$  (T1 (8524-100HF) coded tool,  $Vc=15$  m/min,  $f=0.056$  mm/rev). The most effective parameters on  $Re_{Ti6Al4V}$  were determined as cutting tool geometry, cutting speed and feed rate, with values of 0.001569mm (1.56dB), 0.001398mm (1.38dB) and 0.000646mm (0.73dB), respectively (Table 8).

The main effect graphs indicating the effects of control factors on  $Re_{Ti6Al4V}$  are presented in Fig. 6. The main effect graphs indicating their effects on  $Re_{CFRP}$  are presented in Fig. 6.b. As can be seen in Fig. 6.a, optimum levels of control factors for Ti6Al4V Ti alloy roundness error  $Re_{Ti6Al4V}$  when drilling CFRP/Ti6Al4V metallic stack with different geometry tools,  $Tg1Vc1f2$  (T1 (8524-100HF) coded tool,  $Vc=15$  m/min,  $f=0.056$  mm/rev). In Fig. 6.b, it is seen that the optimum levels for  $Re_{CFRP}$  are  $Tg3Vc1f3$  ( $Tg=T3$  (5514-RT100U) coded tool,  $Vc=15$  m/min,  $f=0.078$  mm/rev). While lower  $Re$  roundness error values were obtained when drilling Ti6Al4V alloy with T1 coded tool, the lowest  $Re$  roundness error values were obtained with T3 coded tool when drilling CFRP. T3 coded tools also yielded lower  $Ra_{CFRP}$  surface roughness ( $Ra_{CFRP}$ ) and lower dimensional accuracy deviation ( $Da_{dev\_CFRP}$ ) values when drilling CFRP (Subtitles 3.1.1 and Subtitles 3.1.2). The T3 coded tool outperforms other cutting tools on  $Re_{CFRP}$  is attributed to the factors explained in detail in Subheading 3.1.1 and Subheading 3.1.2. Lower roundness error values were obtained at the lowest cutting speed when drilling through the metallic stack

in one go [7, 8, 10, 17, 18, 20, 21, 24, 42]. This effect of the cutting speed is attributed to the factors described in detail in Subheading 3.1.1 and Subheading 3.1.2. Again, lower roundness error values were obtained for CFRP and Ti6Al4V components when drilling CFRP/Ti6Al4V mixed metallic stack at medium feed rate ( $f=0.056\text{mm/rev}$ ) and high feed rate ( $f=0.078\text{mm/rev}$ ). However, as shown in the main effect graphs in Fig. 5, lower-dimensional accuracy deviation values were obtained in both CFRP and Ti6Al4V Ti alloys at lower feed rates. A low feed rate is required to obtain a more perfectly dimensionally accurate hole, while a high feed rate is required to obtain holes with a lower roundness error value. When evaluated in terms of hole roundness or roundness error, at a constant cutting speed, while a point on one cutting edge of the cutting tool continues its low-feed linear motion with rotation, it repeatedly touches and erodes the previously machined points on the hole diameter surface along the cutting length in the feed direction. At higher feed rates, while this point on the cutting edge of the drill will continue its linear motion more rapidly along the cutting direction, it will touch less and erode the previously machined points on the hole diameter surface along the cutting length in the feed direction. At low feed rates, the cutting edge of the cutting tool will damage the hole surface more, while at high feed rates, this unnecessary destruction will be eliminated.

ANOVA results of control factors and their interactions for  $Re_{Ti6Al4V}$  and  $Re_{CFRP}$  are presented in Table 9. The most influential factor on  $Re_{Ti6Al4V}$  was the cutting tool geometry-cutting speed interaction ( $Tg*Vc$ ) with a contribution rate of 24.10%. With the contribution ratios of 20.48%, 14.46%, 13.25%, and 10.84%, the cutting tool geo-

metry-cutting speed interaction followed the cutting speed-feed rate interaction ( $Vc*f$ ), the cutting tool geometry ( $Tg$ ), the cutting speed ( $Vc$ ) and the cutting tool geometry-feed rate interaction ( $Tg*f$ ), respectively, (Table 9. a). No statistically significant effect of feed rate on  $Re_{Ti6Al4V}$  was detected. The cutting tool geometry-cutting speed interaction ( $Tg*Vc$ ) was the most effective parameter on  $Re_{CFRP}$  with a contribution rate of 20.56%. The cutting tool geometry-cutting speed interaction was followed by the cutting tool geometry ( $Tg$ ), feed rate ( $f$ ), and cutting speed-feed rate interaction ( $Vc*f$ ), with 18.19%, 15.29%, and 10.64% contribution rates, respectively, (Table 9. b). Other control factors and factor interactions did not significantly affect  $Re_{Ti6Al4V}$  and  $Re_{CFRP}$ .

### 3.3 Multi-Criteria Optimization of Machining Parameters with ARAS Method

With the help of the Taguchi Method, the relationships between control factors and only one quality characteristic can be evaluated. The results of the evaluations performed with the Taguchi Method for each quality characteristic are presented in Section 3.1. The second aim of this experimental work is to determine the optimum combinations of control factors to obtain together minimum surface roughness ( $Ra_{CFRP}$  and  $Ra_{Ti6Al4V}$ ), minimum dimensional accuracy deviation ( $Da_{dev_{CFRP}}$  and  $Da_{dev_{Ti6Al4V}}$ ), and minimum roundness error ( $Re_{CFRP}$  and  $Re_{Ti6Al4V}$ ) in the holes of stack components CFRP and Ti6Al4V in drilling CFRP/Ti6Al4V mixed metallic stacks with different cutting tool geometries and different levels of drilling parameters. For this reason, all calculations and analyses of multi-criteria optimization were made with the ARAS Method.

Table 9. ANOVA results for  $Re_{Ti6Al4V}$  and  $Re_{CFRP}$ .

a) $Re_{Ti6Al4V}$							b) $Re_{CFRP}$						
Source	Degree of Freedom	Sum of Square	Mean Square	F Table	P	Cont. %	Source	Degree of Freedom	Sum of Square	Mean Square	F Table	P	Cont. %
$Tg$	2	0.000012	0.000006	4.15	0.058	14.46	$Tg$	2	0.003545	0.001773	3.04	0.104	18.19
$Vc$	2	0.000011	0.000005	3.73	0.072	13.25	$Vc$	2	0.000823	0.000412	0.71	0.522	4.22
$f$	2	0.000002	0.000001	0.69	0.528	2.41	$f$	2	0.002981	0.00149	2.55	0.139	15.29
$Tg*Vc$	4	0.00002	0.000005	3.47	0.063	24.10	$Tg*Vc$	4	0.004008	0.001002	1.72	0.239	20.56
$Tg*f$	4	0.000009	0.000002	1.54	0.279	10.84	$Tg*f$	4	0.001394	0.000348	0.6	0.675	7.15
$Vc*f$	4	0.000017	0.000004	2.84	0.097	20.48	$Vc*f$	4	0.002073	0.000518	0.89	0.513	10.64
Residual Error	8	0.000012	0.000001			14.46	Residual Error	8	0.004667	0.000583			23.94
Total	26	0.000083				100.00	Total	26	0.019491				100.00

$S=0.001211$   $R^2=85.9\%$   $R^2(\text{adjusted})=54.0\%$

$S=0.02415$   $R^2=76.1\%$   $R^2(\text{adjusted})=22.2\%$

(\*) Statistically significant parameter ( $P<0.05$ )

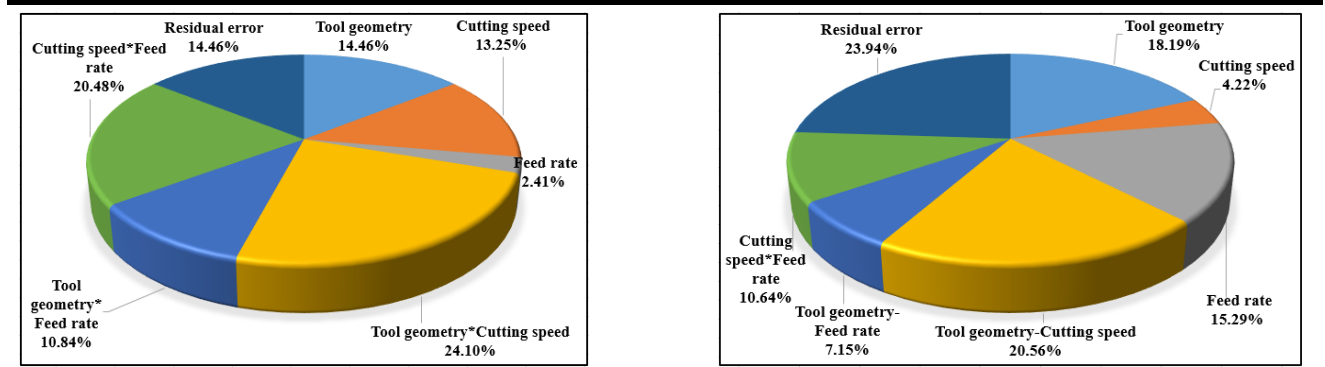


Table 10. Results of ARAS method

Exp No	Dc	f (mm/rev)	Vc (m/min)	Step 1										Step 2				Step 3				Step 4	
				Decision Matrix										Transformed Decision Matrix with Utility Criteria				Weighted Decision Matrix				Optimality Function, Degree of Utility, and Ranking	
				Ra_CFRP	Ra_Ti6Al4V	Da_dev_CFRP	Da_dev_Ti6Al4V	Re_CFRP	Re_Ti6Al4V	Ra_CFRP	Ra_Ti6Al4V	Da_dev_CFRP	Da_dev_Ti6Al4V	Re_CFRP	Re_Ti6Al4V	Ra_CFRP	Ra_Ti6Al4V	Da_dev_CFRP	Da_dev_Ti6Al4V	Re_CFRP	Re_Ti6Al4V	Si	KI
1	15	0.040	0.589	4.733	0.033729	0.543538	0.010341	0.060418	0.0446	0.0391	0.0426	0.0408	0.0286	0.0405	0.0070	0.0035	0.0112	0.0072	0.0026	0.0069	0.0405	0.483030	7
2	15	0.056	0.737	8.234	0.042375	0.836571	0.003783	0.079976	0.0356	0.0226	0.0339	0.0265	0.0511	0.0306	0.0056	0.0032	0.0089	0.0047	0.0046	0.0052	0.0322	0.384844	20
3	15	0.078	1.189	8.318	0.048054	0.918660	0.006629	0.076828	0.0221	0.0223	0.0299	0.0241	0.0446	0.0318	0.0035	0.0032	0.0079	0.0043	0.0040	0.0054	0.0282	0.336941	27
4	21	0.040	0.667	5.913	0.037647	0.557697	0.006992	0.048471	0.0393	0.0314	0.0382	0.0397	0.0423	0.0505	0.0062	0.0045	0.0100	0.0070	0.0038	0.0086	0.0402	0.479272	9
5	21	0.056	0.963	6.719	0.043540	0.692366	0.010060	0.112978	0.0273	0.0276	0.0330	0.0317	0.0294	0.0217	0.0043	0.0039	0.0087	0.0056	0.0026	0.0037	0.0288	0.344241	24
6	21	0.078	0.843	7.226	0.044506	1.314353	0.005761	0.088776	0.0408	0.0257	0.0524	0.0169	0.0513	0.0276	0.0064	0.0036	0.0085	0.0050	0.0046	0.0047	0.0509	0.368923	22
7	29	0.040	0.472	6.301	0.027366	0.458773	0.008270	0.123390	0.0556	0.0295	0.0415	0.0206	0.0385	0.0200	0.0088	0.0042	0.0138	0.0086	0.0032	0.0034	0.0419	0.500370	6
8	29	0.056	0.510	5.681	0.034634	1.073797	0.007674	0.162333	0.0515	0.0327	0.0415	0.0206	0.0385	0.0151	0.0081	0.0046	0.0109	0.0037	0.0035	0.0026	0.0333	0.397915	18
9	29	0.078	0.682	4.677	0.035614	0.638347	0.007610	0.072590	0.0385	0.0397	0.0438	0.0347	0.0389	0.0357	0.0061	0.0056	0.0112	0.0062	0.0035	0.0058	0.0583	0.457480	10
10	15	0.040	0.752	2.727	0.029907	0.627944	0.009564	0.040799	0.0349	0.0681	0.0485	0.0353	0.0309	0.0600	0.0055	0.0096	0.0127	0.0063	0.0028	0.0103	0.0472	0.563211	2
11	15	0.056	0.911	5.942	0.029979	0.970412	0.004886	0.087920	0.0288	0.0313	0.0479	0.0228	0.0430	0.0278	0.0045	0.0044	0.0126	0.0040	0.0039	0.0048	0.0342	0.408496	17
12	15	0.078	1.069	7.459	0.031978	0.958320	0.007795	0.093109	0.0246	0.0249	0.0450	0.0236	0.0379	0.0268	0.0039	0.0035	0.0118	0.0042	0.0034	0.0046	0.0314	0.374515	21
13	21	0.040	0.666	6.023	0.032724	0.911425	0.008315	0.078876	0.0275	0.0304	0.0439	0.0243	0.0356	0.0310	0.0043	0.0044	0.0137	0.0054	0.0038	0.0045	0.0359	0.428228	12
14	21	0.056	0.956	6.119	0.032724	0.911425	0.008315	0.078876	0.0275	0.0304	0.0439	0.0243	0.0356	0.0310	0.0043	0.0044	0.0137	0.0054	0.0038	0.0045	0.0359	0.392533	19
15	21	0.078	0.692	6.420	0.034579	0.780356	0.008902	0.072517	0.0379	0.0289	0.0418	0.0284	0.0352	0.0337	0.0060	0.0041	0.0110	0.0050	0.0030	0.0058	0.0348	0.415870	13
16	29	0.040	0.383	2.644	0.032521	0.690457	0.006901	0.056742	0.0450	0.0703	0.0442	0.0321	0.0429	0.0431	0.0071	0.0100	0.0110	0.0057	0.0039	0.0074	0.0456	0.543871	3
17	29	0.056	0.701	4.740	0.034500	0.844879	0.007732	0.066847	0.0374	0.0392	0.0417	0.0262	0.0383	0.0366	0.0059	0.0056	0.0109	0.0046	0.0034	0.0063	0.0367	0.438487	11
18	29	0.078	0.660	5.689	0.033522	0.349956	0.009179	0.047783	0.0398	0.0327	0.0429	0.0653	0.0322	0.0512	0.0063	0.0046	0.0113	0.0112	0.0029	0.0088	0.0450	0.537451	4
19	15	0.040	0.712	2.603	0.033095	0.726113	0.008960	0.045490	0.0369	0.0714	0.0454	0.0305	0.0350	0.0358	0.0058	0.0101	0.0114	0.0054	0.0030	0.0092	0.0449	0.535871	5
20	15	0.056	0.788	6.733	0.034691	0.651348	0.007046	0.083833	0.0333	0.0276	0.0414	0.0340	0.0420	0.0292	0.0052	0.0039	0.0109	0.0060	0.0038	0.0050	0.0348	0.415726	14
21	15	0.078	0.979	4.491	0.034335	0.441052	0.007404	0.060762	0.0268	0.0414	0.0419	0.0503	0.0400	0.0403	0.0042	0.0059	0.0110	0.0089	0.0036	0.0069	0.0405	0.482905	8
22	21	0.040	0.475	5.095	0.142162	0.399294	0.007641	0.084705	0.0553	0.0365	0.0561	0.0101	0.0555	0.0387	0.0289	0.0087	0.0052	0.0027	0.0098	0.0045	0.0348	0.415164	15
23	21	0.056	0.821	4.256	0.119431	1.093333	0.006459	0.067135	0.0320	0.0456	0.0120	0.0203	0.0438	0.0364	0.0050	0.0062	0.0032	0.0056	0.0041	0.0062	0.0283	0.338069	25
24	21	0.078	0.956	3.172	0.150635	0.161010	0.025540	0.0255	0.0556	0.0110	0.1639	0.0293	0.031	0.0343	0.0083	0.0029	0.0289	0.0026	0.0026	0.0176	0.6647	0.71631	1
25	29	0.040	0.515	5.186	0.046752	0.733125	0.011607	0.071670	0.0510	0.0358	0.0307	0.0302	0.0255	0.0341	0.0080	0.0051	0.0081	0.0054	0.0023	0.0058	0.0347	0.413724	16
26	29	0.056	0.734	5.671	0.055518	1.159950	0.011564	0.075440	0.0358	0.0328	0.0259	0.0191	0.0256	0.0324	0.0056	0.0046	0.0068	0.0034	0.0023	0.0055	0.0283	0.337832	26
27	15	0.040	0.842	7.337	0.050308	0.575192	0.012455	0.071838	0.0312	0.0253	0.0286	0.0385	0.0237	0.0340	0.0049	0.0036	0.0075	0.0068	0.0021	0.0058	0.0308	0.367458	23

All steps are explained in detail in Section 2.3 to determine the optimum drilling parameter combinations; the results are presented in Table 10. Since the optimal values are not fully expressed in the decision matrix to be created using the data of the decision problem, the utility or cost characteristics of the criteria are determined, and the optimal values are determined with the help of Eq.3. The low values (cost situation) of the alternatives for the criteria of *Ti6Al4V*,

*Ra\_CFRP*, *Da\_dev\_Ti6Al4V*, *Da\_dev\_CFRP*, *Re\_Ti6Al4V*, and *Re\_CFRP* are the situations that will positively affect the machinability of the CFRP/Ti6Al4V metallic stack under the most suitable conditions, in other words, it will reduce the total cost. The Decision Matrix, which includes the optimal values calculated by considering the specified criteria, is presented in Table 10.

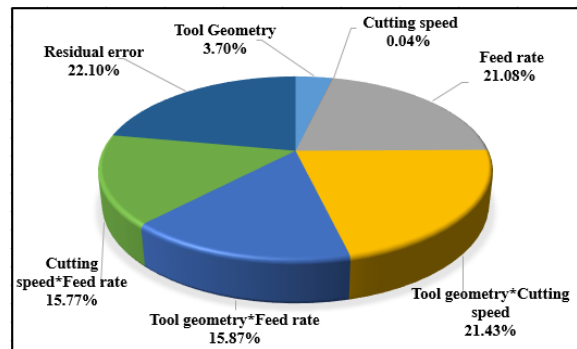
In the second step, the Normalization process was carried out in order to ensure that the alternatives were comparable to the cost-oriented decision matrix created by adding the optimal values determined for  $Ra_{Ti6Al4V}$ ,  $Ra_{CFRP}$ ,  $Da_{dev_{Ti6Al4V}}$ ,  $Da_{dev_{CFRP}}$ ,  $Re_{Ti6Al4V}$  and  $Re_{CFRP}$  in the first step to the data set, to ensure that the alternatives are comparable and to reduce their sizes to lower levels for ease of operation. The criteria' characteristics were also considered in the process of normalizing the performance scores. Since the criteria were required to show cost (minimization) features, the normalization process was completed using Eq. 4 and Eq. 6. The Normalized Decision Matrix was obtained (Table 10). As mentioned in subheading 2.3, 15.76%, 14.17%, 26.25%, 17.72%, 9.0% and 17.11% weight values were determined for  $Ra_{Ti6Al4V}$ ,  $Ra_{CFRP}$ ,  $Da_{dev_{Ti6Al4V}}$ ,  $Da_{dev_{CFRP}}$ ,  $Re_{Ti6Al4V}$  and  $Re_{CFRP}$ , respectively (Table 10). In the third step, the weighted decision matrix expressed by Eq. 8 and Eq. 9 was calculated and presented in Table 10. After the weighted normalized decision matrix was created, the step of calculating the optimality function values for each alternative was started. At this stage, the calculated scores of the alternatives from the criteria were converted to  $S_i$  values using Eq. 10 and  $K_i$  values using Eq. 11. Calculated  $S_i$  and  $K_i$  values and alternative rankings are shown in Table 10. Using the ARAS method, the optimality function values of the alternatives of the process parameters were evaluated from the largest to the smallest, and the alternatives of processing parameters were listed. According to the analysis results, the drilling parameters levels in Experiment No 24 were in the first rank, while the drilling parameters levels in Experiment No 3, which were farthest from optimal, were in the last rank. In this direction, experiment no. 24, which has the ideal processing parameters levels, is close to optimal with a rate of 77.16%. The optimality function value of experiment number 3, the last in the ranking compared to the optimal, was 0.3369, and its similarity to the optimal was determined as 33.69% (Table 10). As a result, the levels of drilling parameters in experiment no. 24 ( $Tg=T3$  (5514-RT100U),  $Vc=21.0$  m/min,  $f=0.078$  mm/rev) were determined as optimal levels via the ARAS method (Table 10).

Finally, ANOVA results for  $K_i$  are presented in Table 11. The ANOVA results in Table 11 reflect the main effects of the process parameters and the effects of their interactions. Considering the ANOVA results in terms of the main effects of the drilling parameters and the effects of their interactions, the order of effectiveness of the drilling parameters in terms of % effect on  $K_i$  (hence minimum  $Ra_{CFRP}$ ,  $Ra_{Ti6Al4V}$ ,  $Da_{dev_{CFRP}}$ ,  $Da_{dev_{Ti6Al4V}}$ ,  $Re_{CFRP}$ , and  $Re_{Ti6Al4V}$ ) was the interaction of cutting tool geometry\*cutting speed ( $Tg*Vc$ ), feed rate ( $f$ ), cutting tool geometry\*feed rate ( $Tg*f$ ), cutting speed\*feed rate ( $Vc*f$ ) with contribution ratios of 21.43%, 21.08%, 15.77%, respectively. The most effective drilling parameter on  $K_i$  was the feed rate (21.08%). It remained below 10% on  $K_i$  of other drilling parameters (Table 11).

Table 11. ANOVA results for  $K_i$ .

a) $Da_{dev_{Ti6Al4V}}$						
Source	Degree of Freedom	Sum of Square	Mean Square	F Table	P	Cont. %
$Tg$	2	0.008498	0.004249	0.67	0.538	3.70
$Vc$	2	0.000096	0.000048	0.01	0.992	0.04
$f$	2	0.048389	0.024194	3.82	0.069	21.08
$Tg*Vc$	4	0.049187	0.012297	1.94	0.197	21.43
$Tg*f$	4	0.036413	0.009103	1.44	0.307	15.87
$Vc*f$	4	0.036197	0.009049	1.43	0.309	15.77
Residual	8	0.050726	0.006341			22.10
Error						22.10
Total	26	0.229506				100.00

$S=0.07963$   $R^2=77.9\%$   $R^2(\text{adjusted})=28.2\%$



#### 4. CONCLUSIONS

The results obtained in this study, in which the effects of cutting tool geometry and machining parameters on surface roughness, deviation from dimensional accuracy, and roundness error in the machining of CFRP/Ti6Al4V metallic composite stacks with coated carbide cutting tools were investigated, and the levels of machining parameters were optimized, are as follows:

- In the drilling of the CFRP component, the surface roughness values of the holes have obtained an average of 641.67% larger than the Ti6Al4V Ti alloy component.
- The best surface quality for the holes in the Ti6Al4V component was obtained with the T1 (8524-100HF), T3 (5514-RT100U), and T2 (2475-100F) coded tools, respectively, while the holes in the CFRP composite component were T3 (5514-RT100U), T2 (2475-100F) and T1 (8524-100HF) coded tools in the drilling of CFRP/Ti6Al4V metallic composite stack,
- Better surface quality was obtained at high cutting speeds and low feed rates when drilling CFRP/Ti6Al4V metallic composite stack. The surface roughness values increase by decreasing the cutting speed and increasing the feed rate.
- Optimal machining conditions were determined as T1(8524-100HF) coded cutting tool,  $Vc=29$ m/min cutting speed, and  $f=0.040$ mm/rev feed rate to obtain minimum  $Ra$  surface roughness value in the Ti6Al4V Ti component. Optimal machining conditions were determined as T3(5514-RT100U) coded tool,  $Vc=29$ m/min cutting speed, and  $f=0.040$ mm/rev feed rate to obtain minimum  $Ra$  surface roughness value in CFRP component.

- The order of influence of machining parameters on the surface roughness of Ti6Al4V Ti component is feed rate (35.26%), cutting speed (25.97%), and cutting speed-feed rate interaction (15.94%). The order of influence of the machining parameters on the surface roughness of the CFRP component is the cutting tool geometry-cutting speed interaction (21.30%), the cutting speed-feed rate interaction (21.11%), and the feed rate (19.77%), and the cutting tool geometry (16.28%).
- While drilling CFRP/Ti6Al4V metallic composite stacks, values closer to the nominal diameter were obtained for the Ti6Al4V component. Compared to the Ti6Al4V Ti alloy, more deviations from the dimensional accuracy of the holes occurred in the drilling of the CFRP component (1481.70%). In contrast, diameter values that deviated considerably from the nominal diameter were obtained in CFRP drilling.
- Values closer to the nominal diameter were obtained with T2 (2475-100F) coded tools for machining Ti6Al4V component and T3 (5514-RT100U) coded tools for drilling CFRP component. Values closer to the nominal diameter were obtained when drilling the Ti6Al4V Ti component at the lowest cutting speed and the CFRP component at the highest cutting speed.
- Values closer to the nominal diameter were obtained when drilling CFRP/Ti6Al4V mixed metallic stack at a low feed rate.
- The order of influence of machining parameters on the deviation from dimensional accuracy in Ti6Al4V Ti component is cutting tool geometry-cutting speed interaction (41.56%), cutting tool geometry (33.19%), and cutting speed (23.29%). The order of influence of the machining parameters on the deviation from dimensional accuracy in the CFRP component is the interaction of cutting tool geometry-feed rate (26.48%), feed rate (18.55%), and cutting tool geometry-cutting speed (14.91%).
- In the drilling of the CFRP/Ti6Al4V mixed metallic stack, the roundness error values of the holes in the CFRP component were found to be 810.47% larger on average than the Ti6Al4V component.
- Values with lower roundness error were obtained with T1 (8524-100HF) coded tools for machining Ti6Al4V component and T3 (5514-RT100U) coded tools for drilling CFRP component.
- Optimal machining conditions were determined as T1(8524-100HF) coded cutting tool,  $V_c=15\text{m/min}$  cutting speed, and  $f=0.056\text{mm/rev}$  feed rate to obtain the minimum hole roundness error value Ti6Al4V Ti component. Optimal machining conditions were determined as T3(5514-RT100U) coded tool,  $V_c=15\text{m/min}$  cutting speed, and  $f=0.078\text{mm/rev}$  feed rate to obtain minimum  $R_a$  surface roughness value in CFRP component.
- The order of influence of machining parameters on the hole roundness error in Ti6Al4V Ti component is cutting tool geometry-cutting speed interaction (24.10%), cutting speed-feed rate interaction (20.48%), cutting tool geometry (14.46%), cutting speed

(13.25%) and cutting tool geometry-feed rate interaction (10.84%), respectively. The order of influence of the machining parameters on the hole roundness error of the CFRP component is the cutting tool geometry-cutting speed interaction (20.56%), the cutting tool geometry (18.19%), the feed rate (15.29%), and the cutting speed-feed rate interaction (10.64%), respectively.

- T3 (5514-RT100U) coded cutting tool,  $V_c=21.0\text{ m/min}$  cutting speed and  $f=0.078\text{ mm/rev}$  CFRP/Ti6Al4V is optimal to obtain minimum surface roughness, dimensional accuracy deviation, and roundness error values when drilling mixed metallic stack with coated carbide tools. Ti6Al4V mixed metallic stacks should be drilled at moderate cutting speeds and higher feed rates to achieve optimum hole quality.

The ARAS method, which was used for multi-objective optimization in this study, can be used in the machinability evaluation of stacks such as CFRP/Al alloy or other processing processes of stacks, apart from machinability evaluation and optimization studies of CFRP/Ti6Al4V mixed metallic stacks because ARAS is a generalized multi-objective optimization method that can be customized for any machining (turning, milling, WEDM, etc.). Therefore, it can effectively optimize the quality characteristics of any production process/product and for other industrial engineering research. In addition, it is thought that the results of this study will contribute to the development of the cutting tool geometry of drilling tools for CFRP or Ti6Al4V Ti alloy materials in practice.

#### FUTURE SCOPE OF WORK

CFRP/Ti6Al4V mixed metallic stacks are frequently used, especially in carrier components of aerospace vehicles. Therefore, the machining and machinability aspect of these stacks is a potential area of research for industries and academia. This study was produced from the project's research results numbered FHD-2020-3211, supported by the Çanakkale Onsekiz Mart University Scientific Research Projects Coordination Unit. Within this project's scope, the machinability of CFRP/Ti6Al4V mixed metallic stacks was evaluated by a multi-criteria optimization method depending on tool geometry, drilling strategy, and cutting parameters. The quality characteristics of the CFRP and Ti6Al4V components of the mixed metallic stack, such as surface roughness, dimensional integrity, circularity error, and delamination formations at the hole entrance and exit of the CFRP during drilling, formed the output variables of the research. In addition, cooling methods, for example, can also affect the quality characteristics of the hole. Factors such as cooling methods, tool wear, material removal mechanics, etc., are among the research planned to be carried out in the future.

#### ACKNOWLEDGEMENT

The authors would like to express their sincere thanks to the Çanakkale Onsekiz Mart University Scientific Research Projects Unit for supporting the project (No. FHD-2020-3211).

## REFERENCES

- [1] Jia, Z.Y., Zhang, C., Wang, F.J. Fu, R.: A mechanistic prediction model for thrust force and torque during drilling of CFRP/Ti stacks, *Int. J. Adv. Manuf.*, Vol. 106, No. 7-8, pp. 3105-3115, 2020.
- [2] Kourra, N., Warnett, J.M., Attridge, A., Dahnel, A., Ascroft, H., Barnes, S. and Williams, M.A.: A metrological inspection method using micro-CT for the analysis of drilled holes in CFRP and titanium stacks, *Int. J. Adv. Manuf.*, Vol. 88, No. 5, pp.1417-1427, 2017.
- [3] Xu, J., An, Q., Ming, W. and Chen, M.: A study on the effects of cutting-sequence strategies in drilling CFRP/Ti, in: *Proceedings of The Advances in Abrasive Technology XX: 20th International Symposium on Advances in Abrasive Technology*, 03-03.12.2017, Okinawa, pp.364-369.
- [4] Motorcu, A.R. and Ekici, E.: CFRP/Ti6Al4V yığının kademeli matkapla delinmesinde CFRP'de minimum delaminasyon faktörü için kontrol faktörlerinin optimizasyonu, in: *Proceedings of The 5. International Conference on Material Science and Technology (IMSTEC 2020)*, 16-18.10.2020, Nevşehir, pp.133-139.
- [5] Motorcu, A.R. and Ekici, E.: CFRP/Ti6Al4V yığının farklı geometri takımlarla delinmesinde minimum delaminasyon oluşumu için proses parametrelerinin çok amaçlı optimizasyonu. in: *Proceedings of The 5th International Congress On Engineering and Technology Management*, 24-25.04.2021, İstanbul, pp.219-231.
- [6] Prasanth, R., Prabukarthi, A., Kumar, M.S., Krishnaraj, V. and Rajamani, R.: identification of drill position in CFRP/Titanium alloy stacks using acoustic emission signals, in: *Proceedings of the International Conference on Advances in Materials, Manufacturing and Applications (AMMA 2015)*, 09-11.04.2015, Trichy, pp.1174-1181.
- [7] Kolesnyk, V., Peterka, J., Kuruc, M., Šimna, V., Moravčíková, J., Vopát, T. and Lisovenko, D.: Experimental study of drilling temperature, geometrical errors and thermal expansion of drill on hole accuracy when drilling CFRP/Ti alloy stacks, *Materials*, Vol. 13, No. 14, pp. 3232, 2020.
- [8] Xu, J. and El Mansori, M.: Experimental study on drilling mechanisms and strategies of hybrid CFRP/Ti stacks, *Compos. Struct.*, Vol. 157, pp. 461-482, 2016.
- [9] Ekici, E. and Motorcu A. R.: CFRP/Ti6Al4V metalik yığının delinmesinde kesme parametreleri ve delme stratejisinin yüzey pürüzlülüğüne etkisi, in: *Proceedings of the 9th International Congress On Engineering, Architecture and Design*, İstanbul, Türkiye, 14-16.05.2022, pp.190-197.
- [10] Xu, J., Zhou, L., Chen, M. and Ren, F.: Experimental study on mechanical drilling of carbon/epoxy composite-Ti6Al4V stacks, *Mater. Manuf. Process.* Vol. 34, No.7, pp.715-725, 2019.
- [11] Xu, J. and El Mansori, M.: Experimental studies on the cutting characteristics of hybrid CFRP/Ti stacks, *Procedia. Manuf.*, Vol. 5, pp. 270-281, 2016.
- [12] Kim, D., Swan, S.R., He, B., Khominich, V., Bell, E., Lee, S.W. and Kim, T.G.: A study on the machinability of advanced arc PVD AlCrN-coated tungsten carbide tools in drilling of CFRP/titanium alloy stacks, *Carbon. Lett.*, Vol. 31, No. 3, pp. 497-507, 2021.
- [13] Isbilir, O. and Ghassemieh, E.: Comparative study of tool life and hole quality in drilling of CFRP/titanium stack using coated carbide drill, *Mach. Sci. Technol.*, Vol. 17, No. 3, pp. 380-409, 2013.
- [14] Zhang, C., Jia, Z., Wang, F., Zhang, B., Bi, G. and Yin, J.: Design of A New One-Shot Tool with Double Margins Structure in Drilling Titanium/Composite Stacks, in: *Proceedings of the 21st International Conference on Composite Materials*, 20-25.08.2017, Xi'an, pp.1-8.
- [15] Wang, B., Wang, Y., Zhao, H., Sun, L., Wang, M. and Kong, X.: Effect of a Ti alloy layer on CFRP hole quality during helical milling of CFRP/Ti laminate, *Compos. Struct.* Vol. 252, pp. 112670, 2020.
- [16] Kayihan, M., Karaguzel, U., Bakkal, M.: Experimental analysis on drilling of Al/Ti/CFRP hybrid composites, *Mater. Manuf. Process.*, Vol. 36, No. 2, pp. 215-222, 2021.
- [17] Xu, J., Ji, M., Chen, M. and El Mansori, M.: Experimental investigation on drilling machinability and hole quality of CFRP/Ti6Al4V stacks under different cooling conditions, *Int. J. Adv. Manuf.*, Vol.109, No. 5, pp. 1527-1539, 2020.
- [18] Xu, J., Ji, M., Chen, M. and Ren, F.: Investigation of minimum quantity lubrication effects in drilling CFRP/Ti6Al4V stacks, *Mater. Manuf. Process.*, Vol. 34, No.12, pp.1401-1410, 2019.
- [19] Akhil, P.V., Krishnaraj, V., Prabukarthi, A., Kumar, M.S. and Elangovan, S.: Study of tool condition monitoring during drilling of CFRP/Ti stacks under dry and wet conditions, in: *Proceedings of the International Conference on Advances in Materials, Manufacturing and Applications (AMMA 2015)*, 09-11.04.2015, Trichy, pp.839-834.
- [20] An, Q., Dang, J., Li, J., Wang, C. and Chen, M.: Investigation on the cutting responses of CFRP/Ti stacks: With special emphasis on the effects of drilling sequences, *Compos. Struct.*, Vol. 253, pp.112794, 2020.
- [21] Jia, Z.Y., Zhang, C., Wang, F.J., Fu, R. and Chen, C.: Multi-margin drill structure for improving hole quality and dimensional consistency in drilling Ti/CFRP stacks, *J. Mater. Process. Technol.*, Vol. 276, pp. 116405, 2020.
- [22] Xu, J., Li, C., Chen, M., El Mansori, M. and Davim, J.P.: On the analysis of temperatures, surface morphologies and tool wear in drilling CFRP/Ti6Al4V stacks under different cutting sequence strategies, *Compos. Struct.*, Vol. 234, pp. 111708, 2020.

- [23] Xu, J., El Mansori, M., Chen, M. and Ren, F.: Orthogonal cutting mechanisms of CFRP/Ti6Al4V stacks, *Int. J. Adv. Manuf.*, Vol. 103, No. 9-12, pp. 3831-3851, 2019.
- [24] Alonso, U., Calamaz, M., Girot, F. and Iriondo, E.: Influence of flute number and stepped bit geometry when drilling CFRP/Ti6Al4V stacks. *J. Manuf. Process.* Vol. 39, pp. 356-370, 2019.
- [25] Prisco, U., Impero, F. and Rubino, F.: Peck drilling of CFRP/titanium stacks: effect of tool wear on hole dimensional and geometrical accuracy, *Prod. Eng.*, Vol. 13, No. 5, pp. 529-538, 2019.
- [26] Kuo, C.L., Soo, S.L., Aspinwall, D.K., Thomas, W., Bradley, S., Pearson, D., M'Saoubi, R. and Leahy, W.: The effect of cutting speed and feed rate on hole surface integrity in single-shot drilling of metallic-composite stacks, *Procedia CIRP*, Vol. 13, pp. 405-410, 2014.
- [27] Ekici, E., Motorcu, A.R., and Uzun, G: Multi-objective optimization of process parameters for drilling fiber metal laminate using a hybrid GRA-PCA approach, *FME Trans.*, Vol. 49 No. 2, pp. 356-366, 2021.
- [28] Pramanik, A. and Littlefair, G.: Developments in machining of stacked materials made of CFRP and titanium/aluminum alloys, *Mach. Sci. Technol.*, Vol. 18, No. 4, pp. 485-508, 2014.
- [29] Shyha, I.S., Soo, S.L., Aspinwall, D.K., Bradley, S., Perry, R., Harden, P. and Dawson, S.: Hole quality assessment following drilling of metallic-composite stacks, *Int. Mach. Tools. Manuf.* Vol. 51, No. 7-8, pp. 569-578, 2011.
- [30] Ashmawi, T.H., Lebrão, G.W., Lebrão, S.M.G. and Bordinassi, É.C.: Study of surface roughness and burr formation after milling of carbon fiber/titanium stacks, *Mater. Res.*, Vol. 22, No. 1, pp. e20190388, 2019.
- [31] Chashchin, N.S., Ivanov, Y.N., Pashkov, A.E. and Sturov, A.A.: (2018). Precise holes machining in multicomponent stacks from metals and CFRP. in: *Proceedings of the International Conference "Aviamechanical engineering and transport" (AVENT 2018)*, 21-26.05.2018, Irkutsk, p.67-72.
- [32] Ekici, E., Motorcu, A.R. and Yıldırım, E.: An experimental study on hole quality and different delamination approaches in the drilling of CARALL, a new FML composite, *FME Trans.*, Vol. 49, No. 4, pp. 950-961, 2021.
- [33] Kumar, J. and Verma, R.K.: Experimental investigations and multiple criteria optimization during milling of Graphene Oxide (GO) doped epoxy/CFRP composites using TOPSIS-AHP hybrid module. *FME Trans.*, Vol. 48, No. 3, pp. 628-635, 2020.
- [34] Nan, C., Wu, D., Gao, Y., Ma, X. and Chen, K.: Influence of metal chips on drilling quality of carbon fiber reinforced plastic and titanium stacks, in: *Proceedings of the IEEE International Conference on Cyber Technology in Automation, Control, and Intelligent Systems (CYBER)*, 08-12.06.2015, Shenyang, p.1204-1209.
- [35] Wei, Y., An, Q., Ming, W. and Chen, M.: Effect of drilling parameters and tool geometry on drilling performance in drilling carbon fiber-reinforced plastic/titanium alloy stacks, *Adv. Mech. Eng.*, Vol. 8, No. 9, pp. 1687814016670281, 2016.
- [36] Kumar, P., Vivek, J., Senniagiri, N., Nagarajan, S. and Chandrasekaran, K.: A study of added SiC powder in kerosene for the blind square hole machining of CFRP using electrical discharge machining, *Silicon*, Vol. 14, pp. 1831-1849, 2022.
- [37] Paramasivam, S.S.S.S., Kumaran, D. and Natarajan, H.: Taguchi Additive Ratio Assessment (ARAS) method in multi-criteria decision making: A case study for treated drill tools performance. *Int. J. Mod. Manuf.*, Vol.12, No.1, pp.114-124, 2020.
- [38] Yıldırım, B.F.: Çok kriterli karar verme problemlerinde ARAS yöntemi, *Kafkas Üniversitesi İktisadi ve İdari Bilimler Fakültesi Dergisi*, Vol. 6, No. 9, pp. 285-296, 2015.
- [39] Ji, M., Xu, J., Chen, M. and Mansori, M.E.: Effects of different cooling methods on the specific energy consumption when drilling CFRP/Ti6Al4V stacks, *Procedia Manuf.* Vol. 43, pp. 95-102, 2020.
- [40] Xu, J., El Mansori, M., Voisin, J., Chen, M. and Ren, F.: On the interpretation of drilling CFRP/Ti6Al4V stacks using the orthogonal cutting method: Chip removal mode and subsurface damage formation, *J. Manuf. Process.*, Vol. 44, pp. 435-447, 2019.
- [41] Wang, Q., Wang, F., Zhang, C. and Chen, C.: Combined effects of various materials on tool wear in drilling of Ti/CFRP stacks, *Proc. Inst. Mech. Eng. C. J. Mech. Eng. Sci.*, Vol. 234, No. 14, pp. 2750-2759, 2020.
- [42] Kumar, D., Gururaja, S. and Jawahir, I.S.: Machinability and surface integrity of adhesively bonded Ti/CFRP/Ti hybrid composite laminates under dry and cryogenic conditions, *J. Manuf. Process.*, Vol. 58, pp. 1075-1087, 2020.
- [43] Jia, Z.Y., Zhang, C., Wang, F.J., Fu, R. and Chen, C.: An investigation of the effects of step drill geometry on drilling induced delamination and burr of Ti/CFRP stacks, *Compos. Struct.* Vol. 235, pp. 111786, 2020.

---

**ПРОЦЕНА И ВИШЕКРИТЕРИЈУМСКА  
ОПТИМИЗАЦИЈА ХРАПАВОСТИ  
ПОВРШИНЕ, ОДСТУПАЊА ОД ТАЧНОСТИ  
ДИМЕНЗИЈА И ГРЕШКЕ ЗАОБЉЕНОСТИ У  
БУШЕЊУ CFRP/Ti6Al4V НАСЛАГА**

**А.Р. Моторчу, Е. Екичи**

У овој студији спроведени су тестови обрадивости како би се истражили утицаји контролних фактора (геометрија резног алата, брзина резања и брзина помака) на храпавост површине (Ra), одступање од тачности димензија (Da<sub>dev</sub>), грешку заобљености (Re) у бушење CFRP/Ti6Al4V мешаног металног слоја и за одређивање оптималних нивоа параметара бушења. Анализирани су ефекти сваког контролног фактора и њихове интеракције на три

карактеристике квалитета, а њихови нивои су једнообјективно оптимизовани за сваки компонентни материјал Тагучи методом. Материјал има компоненте (CFRP и Ti6Al4V) са суштински различитим особинама (механичке, физичке, обрадивост). Оптимизација са једним циљем има ограничену употребљивост јер се бушење мора извршити у једном кроз оба слоја. Стога, у додатном кораку, оптимални нивои контролних

фактора су одређени оптимизацијом вишеструких циљева методом Аддитиве Ратио Ассесмент (ARAS). Више вредности Ra, Da\_дев и Re су добијене на компоненти CFRP у поређењу са компонентом Ti6Al4V. CFRP/Ti6Al4V стог треба да се избуши са нано ватром обложеном карбидном сврдлом (T3) при средњој брзини сечења и великом брзином помака да би се постигле минималне вредности Ra, Da\_DEV и Re у једном потезу.